

Modeling of bending-torsion couplings in active-bending structures. Application to the design of elastic gridshell.



École des Ponts
ParisTech

Thèse n. xxxxx
présenté le 01 décembre 2017
à l'Ecole des Ponts ParisTech
laboratoire Navier
Université Paris-Est

pour l'obtention du grade de Docteur ès Sciences
par

Lionel du Peloux

acceptée sur proposition du jury:

Prof Name Surname, président du jury
Prof Name Surname, directeur de thèse
Prof Name Surname, rapporteur
Prof Name Surname, rapporteur
Prof Name Surname, rapporteur

Paris, Ecole des Ponts ParisTech, 2016

Contents

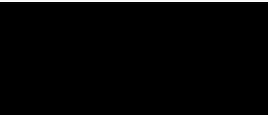
Contents	i
List of Figures	iii
List of Tables	v
3 Geometry of smooth and discrete space curves	1
3.1 Introduction	1
3.1.1 Overview	1
3.1.2 Contributions	2
3.1.3 Related work	3
3.2 Parametric curves	4
3.2.1 Definition	4
3.2.2 Regularity	4
3.2.3 Reparametrization	5
3.2.4 Natural parametrization	5
3.2.5 Curve length	5
3.2.6 Arc length parametrization	5
3.3 Frenet trihedron	6
3.3.1 Tangent vector	6
3.3.2 Normal vector	7
3.3.3 Binormal vector	8
3.3.4 Osculating plane	9
3.4 Curves of double curvature	9
3.4.1 First invariant : the curvature	10
3.4.2 Second invariant : the torsion	12
3.4.3 Fundamental theorem of space curves	12
3.4.4 Serret-Frenet formulas	13
3.5 Curve framing	14
3.5.1 Moving frame	15
3.5.2 Adapted moving frame	17
3.5.3 Rotation-minimizing frame	18
3.5.4 Parallel transport	18

Contents

3.5.5	Frenet frame	19
3.5.6	Bishop frame	21
3.5.7	Comparison between Frenet and Bishop frames	23
3.6	Discrete curves	25
3.6.1	Definition	25
3.6.2	Regularity	26
3.6.3	Parametrization	27
3.7	Discrete curvature	28
3.7.1	Definition from osculating circles	28
3.7.2	Benchmarking : sensitivity to non uniform discretization	31
3.7.3	Benchmarking : accuracy in bending energy representation	33
3.8	Discrete tangent vector	36
3.8.1	Circumscribed case	37
3.8.2	Inscribed case	39
3.9	Discrete parallel transport	43
3.9.1	The rotation method	43
3.9.2	The double reflexion method	43
3.10	Conclusion	45
3.11	References	46

List of Figures

3.1	Definition of the tangent vector and the osculating circle of a curve	7
3.2	Osculating circles for a spiral curve at different parameters	10
3.3	Discontinuity of the Frenet trihedron at an inflexion point	14
3.4	Geometric interpretation of the angular velocity vector of a moving frame .	16
3.5	Adapted moving frame on a circular helix	17
3.6	Angular velocities of Frenet and Bishop frames for a circular helix	24
3.7	Discrete curve representation and parametrization	26
3.9	Comparison of circumscribed and inscribed osculating circles	32
3.10	Sensitivity of discrete curvatures to non uniform discretization	32
3.11	Discretization of a semicircle and evaluation of its bending energy	34
3.12	Relative error in the estimation of the bending energy of a semicircle	34
3.13	Discretization of an elastica curve and evaluation of its bending energy . . .	35
3.14	Relative error in the estimation of the bending energy of an elastica	35
3.15	Definition of the tangent vector associated to the circumscribed curvature .	38
3.16	Definition of the tangent vector associated to the inscribed curvature	40
3.17	Two methods to parallel transport a vector	44



List of Tables

3.1	Review of several discrete curvature definitions	29
-----	--	----

3 Geometry of smooth and discrete space curves

3.1 Introduction

In this chapter, our goal is to develop a comprehensive view of the geometry of space curves and how to frame such curves. Indeed, framed curve representations are of central importance when dealing with slender beam models, as they are often modeled using curvilinear coordinate systems. This is the kind of representation on which our beam model will be based on.

Although the theoretical beam model takes place in the smooth world, our model will be implemented in a numerical solver, hence the necessity of a discrete representation. However, the two world are intimately related to each other and this is why we chose to present them both in this chapter.¹

A comprehensive understanding of the geometry of discrete curves will enable to build a beam model with reduced degrees of freedom and capable of representing discontinuities in curvature. This last point is of particular interest when modeling real structures with complex boundary conditions and connexions where concentrated moments are transferred (that is jumps in curvature occur).

3.1.1 Overview

We start this chapter by recalling the fundamentals of smooth parametric curves (see §3.2). We introduce the *Frenet frame*, a crucial tool for the local characterization of space curves (see §3.3), and we identify two geometric invariants, the curvature and the torsion of Frenet,

¹de L'Hospital 1696 [1, preface] : “Car les courbes n’étant que des polygones d’une infinité de côtés, & ne différant entr’ elles que par la différence des angles que ces côtés infiniment petits font entr’eux ; il n’appartient qu’à l’Analyse des infiniment petits de déterminer la position de ces cotés pour avoir la courbure qu’ils forment [...]”.

that fully describe the geometry of a given space curve (see §3.4). We then introduce the notion of moving frame which allow to define a local orientation to each material point on a curve (see §3.5). This description will later be essential when modeling cross-section of beams. Among all the possible ways to frame a curve we look at rotation-minimizing frames. These frames are constructed thanks to the parallel transport operator, defined in the same section, which leads to the introduction of the *Bishop frame* : a torsion-free moving frame that will be at the heart of the beam model developed in the following chapters.

We then move on the discrete case and we first draw up a representation of a discrete curve as an ordered sequence of vertices linked by edges (see §3.6). We gather several definitions of the curvature for a discrete curve and we interpret them in terms of their osculating circle (see §3.7). Among these definitions, we focus on the curvatures defined respectively by the circumscribed and the inscribed osculating circles. We extend their definition to the curve endings as this is a matter of concern when dealing with mechanical boundary conditions – such as pinned or fixed endings. We study their behavior with respect to the turning angle – that is the angle between two consecutive edges – and we analyze their sensitivity to non uniform discretizations as this is a matter of concern when modeling real structures (see §3.7.2). We then compare to what extent these curvatures can represent accurately the bending energy of typical curves, namely a circular curve and an elastica curve (see §3.7.3). For these two curvatures we demonstrate that a natural definition for the tangent vector emerges and we show how to construct it all along the discrete curve. This vector will later be associated to the cross-section normal in our Kirchhoff beam model (see §3.8). Finally, we recall two methods to parallel transport vectors or frames along a discrete curve (see §3.9). These methods will be used later to construct a twist-free reference frame for our beam model.

3.1.2 Contributions

- We gather several definitions of the curvature for a discrete curve and we interpret them in terms of their osculating circle.
- We focus on the discrete curvatures defined respectively by the circumscribed and the inscribed osculating circles. We extend their definition to curve endings, which is crucial when modeling mechanical boundary conditions where nodes are positioned at points of interest.
- We study their behavior with respect to the turning angle and we analyze their sensitivity to non uniform discretization, which is likely to arise when modeling real structures.
- We compare to what extent these curvatures can represent accurately the bending energy of typical bended shapes (circle and elastica) regarding the sharpness of the discretization. This help us to chose what curvature representation to implement in our beam model.
- We demonstrate that a natural definition for the tangent vector at vertices emerges

for these curvatures. This will lead to a model with reduced number of degrees of freedom.

- We show how the local curvature and the tangent vector are related one to each other. This will lead to a straightforward modeling of boundary conditions and connexions. This will also allow to model discontinuities in curvature at vertices, thus enabling the modeling of applied concentrated moment and jumps in beam properties (ES , EI , GJ).

3.1.3 Related work

Delcourt 2011 [2] gives a thorough historical review of the study of space curves from Clairaut to Darboux. This history is paved with the nouns of illustre mathematicians such as Euler, Bernoulli, Monge, Fourier, Lagrange, Cauchy, Serret, Frenet, . . . It reveals that the study of curves was often related to the study of physical problems (e.g. the elastica for Bernoulli & Euler, the helix for Pito).

In his lecture notes on discrete differential geometry of curves and surfaces, Hoffmann 2008 [3] presents three definitions for the discrete curvature. In his lecture notes on discrete differential geometry of plane curves, Vouga 2014 [4] constructs new discrete curvatures that mimic some of the interesting properties of the curvature in the smooth case. He remarks that none of the established discrete curvatures can reproduce all the properties of the curvature in the smooth case.

Bishop 1975 [5] remarks that the usual Frenet frame is not the only way to frame curve. He gives the skew-symmetric system of differential equations that any moving frame satisfies. He remarks that this system is governed by only three coefficient entries, which represent the components of the angular velocity vector of the frame expressed on the frame axes. He argues that the Frenet frame gains part of its significance because it is adapted to the curve and because one component of its angular velocity is null. Hence, he looks for other kind of moving frames that are both adapted and with one of the components of the angular velocity vector that is null. In particular, he looks at adapted frames that does not turn around the curve : what will be called a Bishop frame hereafter.

Klok 1986 [6] makes use of the Bishop frame to produce rotation-minimizing sweeps for visualizing 3D ribbons and cylinders. He remarks that for closed trajectories the start and end frames might not align properly. Guggenheimer 1989 [7] proposes a faster method to compute Klok's frame in relation to the Frenet frame. For that, he remarks that any frame is obtained from the Frenet frame by a rotation around the tangent vector. Bloomenthal 1990 [8] introduces the rotation method to propagate reference frames along a curve. Hanson and Ma 1995 [9] propose an algorithm to parallel transport frames along a curve using the rotation method. Poston et al. 1995 [10] propose a quadratically convergent algorithm, also based on the rotation method, to find untwisted sweeping NURBS surfaces within a given error bound ϵ .

Wang et al. 2008 [11] introduce the double reflexion method to propagate rotation min-

imizing frames. This method is supposed to be more stable than the rotation method Farouki et al. 2014 [12] investigate the use of rotation-minimizing frames that minimize the rotation around the binormal vector of the curve (compare to Bishop frame that minimize the rotation around the tangent vector of the curve).

3.2 Parametric curves

In this section we recall some fundamental results on (smooth) parametric curves.² In particular, we recall that there is more than one way to parametrize a curve. Amongst all the possible ways to parametrize a given curve, the arc length parametrization is of special interest. With this parametrization, the way a curve is described by a single parameter becomes unequivocal.³ This parametrization is naturally related to what is commonly understood as the “length of a curve”.

3.2.1 Definition

Let I be an interval of \mathbb{R} and $F: t \mapsto F(t)$ be a map of $\mathcal{C}^0(I, \mathbb{R}^3)$. Then $\gamma = (I, F)$ is called a *parametric curve* and :

- The 2-uplet (I, F) is called a *parametrization* of γ .
- $\gamma = F(I) = \{F(t), t \in I\}$ is called the *graph* or *trace* of γ .
- γ is said to be \mathcal{C}^k if $F \in \mathcal{C}^k(I, \mathbb{R}^3)$.⁴

Note that for a given graph in \mathbb{R}^3 there are different possible parameterizations. Thereafter γ will simply refers to its graph $F(I)$.

3.2.2 Regularity

Let $\gamma = (I, F)$ be a parametric curve, and $t_0 \in I$ be a parameter.

- A point of parameter t_0 is called *regular* if $F'(t_0) \neq 0$.
The curve γ is called *regular* if γ is \mathcal{C}^1 and $F'(t) \neq 0, \forall t \in I$.
- A point of parameter t_0 is called *biregular* if $F'(t_0)$ and $F''(t_0)$ are not collinear.
The curve γ is called *biregular* if γ is \mathcal{C}^2 and $F'(t) \times F''(t) \neq 0, \forall t \in I$.

²Definition from [mathworld](#) : “A smooth curve is a curve which is a smooth function, where the word ‘curve’ is interpreted in the analytic geometry context. In particular, a smooth curve is a continuous map from a one-dimensional space to an n-dimensional space which on its domain has continuous derivatives up to a desired order.”.

³This is not rigorously exact but that is the idea. Indeed, this is true only for a given choice of orientation and to within a constant.

⁴A function f is said to be of class \mathcal{C}^k if $f, f', f'', \dots, f^{(k)}$ exist and are continuous.

Here and thereafter, the prime symbol denotes the derivation with respect to the parameter and the product symbol denotes the cross product.

3.2.3 Reparametrization

Let $\gamma = (I, F)$ be a parametric curve of class \mathcal{C}^k , $J \in \mathbb{R}^3$ an interval, and $\varphi: I \mapsto J$ be a \mathcal{C}^k diffeomorphism. Let's define $G = F \circ \varphi$. Then :

- $G \in \mathcal{C}^k(J, \mathbb{R}^3)$
- $G(J) = F(I)$
- φ is said to be an admissible *change of parameter* for γ .
- (J, G) is said to be another *admissible parametrization* for γ .

3.2.4 Natural parametrization

Let γ be a space curve of class \mathcal{C}^1 . A parametrization (I, F) of γ is called *natural* if $\|F'(t)\| = 1, \forall t \in I$. Thus :

- The curve is necessarily regular.
- F is strictly monotonic.

3.2.5 Curve length

Let $\gamma = (I, F)$ be a parametric curve of class \mathcal{C}^1 . The length of γ is defined as :

$$L = \int_I \|F'(t)\| dt \tag{3.1}$$

Note that as expected, the length of γ is invariant under reparametrization.

3.2.6 Arc length parametrization

Let $\gamma = (I, F)$ be a regular parametric curve. Let $t_0 \in I$ be a given parameter. The following map is said to be the *arc length of origin* t_0 of γ :

$$s: t \mapsto \int_{t_0}^t \|F'(u)\| du \quad , \quad s \in I \times \mathbb{R} \tag{3.2}$$

The arc length $s: I \mapsto s(I)$ is an admissible change of parameter for γ . Indeed, s is a \mathcal{C}^1 diffeomorphism because it is bijective ($s' > 0$).

Let's define $G = F \circ s^{-1}$ and $J = s(I)$. Thus (J, G) is a natural reparametrization of γ and $\forall s \in J, \|G'(s)\| = 1$. This parametrization is preferred because the natural parameter s

traverses the image of γ at unit speed ($\|G'\| = 1$).⁵

Thereafter, for a regular curve γ , $\gamma(t)$ will denote the point $F(t)$ of parameter $t \in I$ while $\gamma(s)$ will denote the point $G(s)$ of arc length $s \in J = [0, L]$.

3.3 Frenet trihedron

The Frenet trihedron is a fundamental mathematical tool from the field of differential geometry to study the local characterization of planar and non-planar space curves. It is a direct orthonormal basis attached to any point P of parameter $t \in I$ on a parametric curve γ . This basis is composed of three unit vectors $\{\mathbf{t}(t), \mathbf{n}(t), \mathbf{b}(t)\}$ called respectively the *tangent*, the *normal*, and the *binormal* unit vectors.⁶

Introduced by Frenet in 1847 in his thesis “Courbes à Double Courbure” [13], it brings out intrinsic local properties of space curves : the curvature (κ) which evaluates the deviance of γ from being a straight line (see §3.4.1) ; and the torsion (τ_f) which evaluates the deviance of γ from being a planar curve (see §3.4.2).

These quantities, also known as “generalized curvatures” in modern differential geometry, are essential to understand the geometry of space curves. As stated by the *Fundamental Theorem of Space Curves*,⁷ a curve is fully determined by its curvature and torsion up to a solid movement in space (see §3.4.3).

3.3.1 Tangent vector

The first component of the Frenet trihedron is called the *unit tangent vector*. Let $\gamma = (I, F)$ be a regular parametric curve. Let $t \in I$ be a parameter. The *unit tangent vector* is defined as :

$$\mathbf{t}(t) = \frac{\gamma'(t)}{\|\gamma'(t)\|} \quad , \quad \|\mathbf{t}(t)\| = 1 \quad (3.3)$$

For a curve parametrized by arc length, this expression simply becomes :

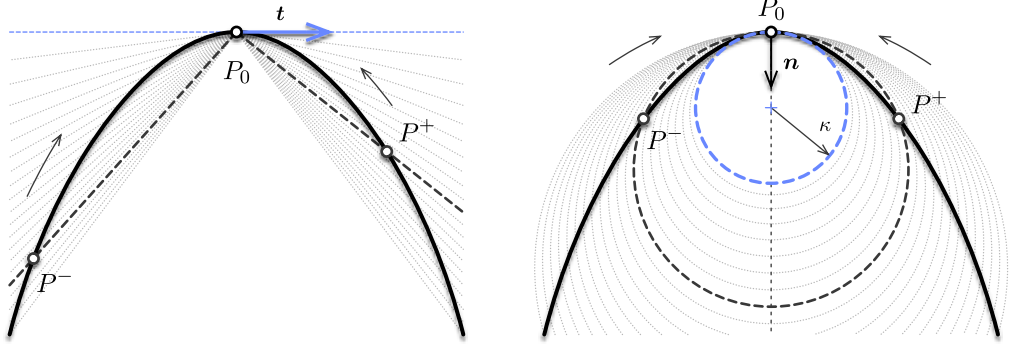
$$\mathbf{t}(s) = \gamma'(s) \quad , \quad s \in [0, L] \quad (3.4)$$

In differential geometry, the unit tangente to the curve γ at point P_0 is obtained as the limit of the (normalized) vector $\overrightarrow{P_0 P}$, when P approaches P_0 on the path γ (see fig. 3.1). For a regular curve, the left-sided and right-sided limits coincide as P^- and P^+ approche

⁵Regular curves are also known as *unit speed* curves.

⁶ Strictly speaking the map $\mathbf{t} : t \mapsto \mathbf{t}(t)$ is a *vector field* while $\mathbf{t}(t)$ is a *vector* of \mathbb{R}^3 . For the sake of simplicity, and if there is no ambiguity, these two notions will not be explicitly distinguished hereinafter.

⁷The full demonstration of this theorem is attributed to Darboux in [14, p.11].



(a) Curve's tangent.

(b) Curve's normal and osculating circle.

Figure 3.1 – Definition of the tangent vector and the osculating circle of a curve.

P_0 respectively from its left and right sides :

$$\mathbf{t}(P_0) = \lim_{P \rightarrow P_0} \frac{\overrightarrow{P_0 P}}{\|\overrightarrow{P_0 P}\|} = \lim_{P^- \rightarrow P_0} \frac{\overrightarrow{P_0 P^-}}{\|\overrightarrow{P_0 P^-}\|} = \lim_{P^+ \rightarrow P_0} \frac{\overrightarrow{P_0 P^+}}{\|\overrightarrow{P_0 P^+}\|} \quad (3.5)$$

3.3.2 Normal vector

The second component of the Frenet trihedron is called the *unit normal vector*. It is constructed from \mathbf{t}' which is necessarily orthogonal to \mathbf{t} . Indeed :

$$\|\mathbf{t}\| = 1 \Rightarrow \mathbf{t}' \cdot \mathbf{t} = 0 \Leftrightarrow \mathbf{t}' \perp \mathbf{t} \quad (3.6)$$

Remark that for a curve parametrized by arc length [eq. \(3.6\)](#) implies that $\gamma'(s) \cdot \gamma''(s) = 0$.

Let $\gamma = (I, F)$ be a biregular parametric curve. Let $t \in I$ be a parameter. The *unit normal vector* is defined as : ⁸

$$\mathbf{n}(t) = \frac{\mathbf{t}'(t)}{\|\mathbf{t}'(t)\|}, \quad \|\mathbf{n}(t)\| = 1 \quad (3.7)$$

Using [eq. \(3.3\)](#) in [eq. \(3.7\)](#) plus the usual derivation rules leads to : ⁹

$$\mathbf{t}'(t) = \frac{\gamma'(t) \times (\gamma''(t) \times \gamma'(t))}{\|\gamma'(t)\|^3} \quad (3.8)$$

⁸Note that \mathbf{n} exists if only γ is biregular, that is \mathbf{t}' never vanishes, or equivalently γ is never locally a straight line. In that case the Frenet trihedron is undefined.

⁹Recall that $\gamma'(t) \times (\gamma''(t) \times \gamma'(t)) = \gamma''(t)(\gamma'(t) \cdot \gamma'(t)) - \gamma'(t)(\gamma''(t) \cdot \gamma'(t))$ and that $\|\gamma'(t)\| = \sqrt{\gamma'(t) \cdot \gamma'(t)}$.

Because $\gamma'(t)$ and $\gamma''(t) \times \gamma'(t)$ are perpendicular the following identity holds :

$$\|\gamma'(t) \times (\gamma''(t) \times \gamma'(t))\| = \|\gamma'(t)\| \|\gamma''(t) \times \gamma'(t)\| \quad (3.9)$$

Thus, combining eq. (3.8) and (3.9) gives :

$$\mathbf{n}(t) = \frac{\gamma'(t) \times (\gamma''(t) \times \gamma'(t))}{\|\gamma'(t)\| \|\gamma''(t) \times \gamma'(t)\|} \quad (3.10)$$

For a curve parametrized by arc length this expression becomes :

$$\mathbf{n}(s) = \frac{\gamma''(s)}{\|\gamma''(s)\|} \quad , \quad s \in [0, L] \quad (3.11)$$

In differential geometry, the unit normal to the curve γ at point P_0 is obtained as the limit of the (normalized) vector $\overrightarrow{P_0 P^+} - \overrightarrow{P_0 P^-}$, as P^- and P^+ approach P_0 respectively from its left and right sides (fig. 3.1) :

$$\mathbf{n}(P_0) = \lim \frac{\overrightarrow{P_0 P^+} - \overrightarrow{P_0 P^-}}{\|\overrightarrow{P_0 P^+} - \overrightarrow{P_0 P^-}\|} \quad (3.12)$$

Remark that the notion of *normal vector* is ambiguous for non-planar curves as there is an infinite number of possible normal vectors lying in the plane orthogonal to the curve's tangent. In practice, the tangent derivative is a convenient choice as it allows to extend the notion of curvature from planar to non-planar space curves. However, we will see in §3.5.6 that other kinds of trihedron can be constructed regarding this choice and that one of them is especially suitable for the study of slender beams.

3.3.3 Binormal vector

The third vector of Frenet's trihedron is called the *unit binormal vector*. It is constructed from \mathbf{t} and \mathbf{n} to form an orthonormal direct basis of \mathbb{R}^3 . Let $\gamma = (I, F)$ be a biregular parametric curve. Let $t \in I$ be a parameter. The *unit binormal vector* is defined as :

$$\mathbf{b}(t) = \mathbf{t}(t) \times \mathbf{n}(t) \quad , \quad \|\mathbf{b}(t)\| = 1 \quad (3.13)$$

Combining eq. (3.3) and eq. (3.10) with eq. (3.13) leads to :

$$\mathbf{b}(t) = \frac{\gamma'(t) \times \gamma''(t)}{\|\gamma'(t) \times \gamma''(t)\|} \quad (3.14)$$

For a curve parametrized by arc length, this expression becomes : ¹⁰

$$\mathbf{b}(s) = \mathbf{t}(s) \times \mathbf{n}(s) = \frac{\gamma'(s) \times \gamma''(s)}{\|\gamma''(s)\|} \quad , \quad s \in [0, L] \quad (3.15)$$

¹⁰For an arc length parametrized curve the following identity holds : $\|\gamma'(s) \times \gamma''(s)\| = \|\gamma'(s)\| \|\gamma''(s)\|$.

3.3.4 Osculating plane

The tangent and normal unit vectors $\{\mathbf{t}, \mathbf{n}\}$ form an orthonormal basis of the so-called *osculating plane*, whereas the binormal vector (\mathbf{b}) is orthogonal to it. This plane is of prime importance because it is the plane in which the curve takes its curvature (see §3.4.1).

As reported in [14, p.45], the osculating plane seems to have been first introduced by Bernoulli as the plane passing through three infinitely near points on a curve.¹¹ Likewise, in modern differential geometry, the osculating plane is defined as the limit of the plane passing through the points P^- , P_0 and P^+ while P^- and P^+ approach P_0 respectively from its left and right side (fig. 3.1).

Note that the normal unit vector and the binormal unit vector $\{\mathbf{n}, \mathbf{b}\}$ define the so-called *normal plane*, while the normal tangent vector and the binormal unit vector $\{\mathbf{t}, \mathbf{b}\}$ define the so-called *rectifying plane*. These planes are secondary for the present study.

3.4 Curves of double curvature

The study of space curves belongs to the field of differential geometry. According to [14, p.28], the terminology *curve of double curvature* is attributed to Pitot around 1724.¹² However, as stated in [17, p.321] curvature and torsion were probably first thought by Monge around 1771.¹³ It is also interesting to note that, at that time, “curvature” was also referred to as “flexure”, reflecting that the study of physical problems (e.g. *the elastica*) and the study of curves of double curvature were intimately related to each other.

Space curves were historically understood as *curves of double curvature* by extension to the case of planar curves, where the curvature measures the deviance of a curve from being a straight line. The second curvature, nowadays known as the “torsion” or “second generalized curvature”, measures the deviance of a curve from being planar.

¹¹“Voco autem planum osculans, quod transit per tria curvae quaesitae puncta infinite sibi invicem propinqua” [15, p.113].

¹²“Les Anciens ont nommé cette courbe Spirale ou Hélice ; parce que la formation sur le cylindre suit la même analogie que la formation d’une spirale ordinaire sur un plan; mais elle est bien différente de la spirale ordinaire, étant une des courbes à double courbure, ou une des lignes qu’on conçoit tracée sur la surface des Solides. Peut-être que ces sortes de courbes à double courbure, ou prises sur la surface des Solides, feront un jour l’objet des recherches des géomètres. Celle que nous venons d’examiner est, je crois, la plus simple de toutes. ” [16, p.28]

¹³“On appelle point d’inflexion, dans une courbe plane, le point où cette ligne, après avoir été concave dans un sens, cesse de l’être pour devenir concave dans l’autre sens. Il est évident que dans ce point, la courbe perd sa courbure, et que les deux élémens consécutifs sont en ligne droite. Mais une courbe à double courbure peut perdre chacune de ses courbures en particulier, ou les perdre toutes deux dans le même point ; c’est-à-dire, qu’il peut arriver ou que trois élémens consécutifs d’une même courbe à double courbure se trouvent dans un même plan, ou que deux de ces élémens soient en ligne droite. Il suit de là que les courbes à double courbure peuvent avoir deux espèces d’inflexions ; la première a lieu lorsque la courbe devient plane, et nous l’appellerons simple inflexion ; la seconde, que nous appellerons double inflexion, a lieu lorsque la courbe devient droite dans un de ses points.” [18, p.363].

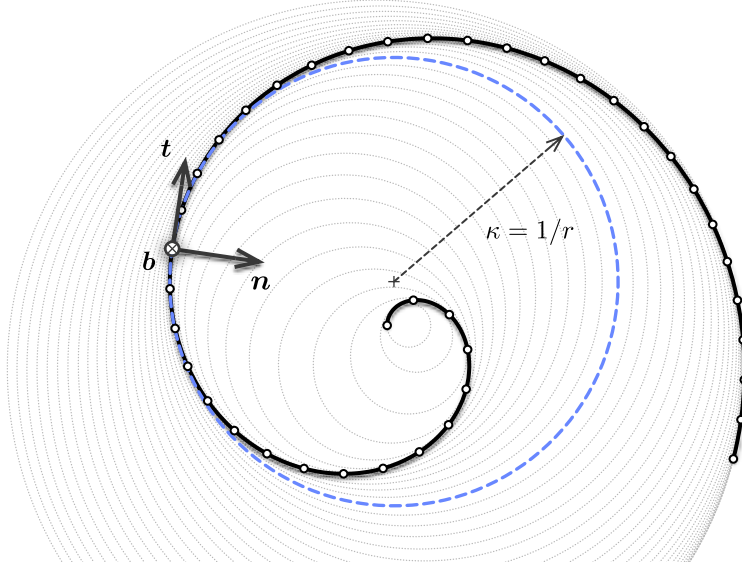


Figure 3.2 – Osculating circles for a spiral curve at different parameters.

3.4.1 First invariant : the curvature

In differential geometry, the *osculating circle* is defined as the limit of the circle passing through the points P^- , P_0 and P^+ while P^- and P^+ approach P_0 (fig. 3.1). This circle lies on the osculating plane and its radius is nothing but the inverse of the local curvature of a curve.¹⁴ While the tangent gives the best local approximation of the curve as a straight line, the osculating circle gives the best local approximation of that curve as an arc.

The curvature is also known to be the *gradient of arc length* (see [4, p.4]) and calculated as : $\nabla L = \kappa \mathbf{n}$. Thus, the curvature gives the first-order variation in arc length when deforming a curve γ into the curve $\gamma + \epsilon \delta \gamma$:

$$L(\gamma + \epsilon \delta \gamma) = L(\gamma) + \epsilon (\nabla L \cdot \delta \gamma) + o(\epsilon) \quad (3.16a)$$

$$\nabla L \cdot \delta \gamma = \left. \frac{d}{d\epsilon} L(\gamma + \epsilon \delta \gamma) \right|_{\epsilon=0} = \int_0^L \kappa (\delta \gamma \cdot \mathbf{n}) \quad (3.16b)$$

This is easily understood in the case of a circle of radius r extended to a circle of radius $r + dr$, where the total arc length variation is given by : $L(r + dr) - L(r) = \kappa dr L(r)$.

Note that due to the inner product with the normal vector, only the normal component of the deformation results in an effective extension of the curve. This point is worth to note as it will be related to the *inextensibility assumption* made later in our beam model (see ??).

¹⁴As explained by Euler himself, at a given arc length parameter (s), the osculating plane is the plane in which a curve takes its curvature : “in quo bina fili elementa proxima in curvantur” [19, p.364].

Curvature

Let γ be a regular arc length parametrized curve. Let $s \in [0, L]$ be an arc length parameter. The *curvature* is a positive scalar quantity defined as :

$$\kappa(s) = \|\mathbf{t}'(s)\| \geq 0 \quad , \quad \mathbf{t}'(s) = \kappa(s)\mathbf{n}(s) \quad (3.17)$$

The curvature is *independent* regarding the choice of parametrization. This makes the curvature an *intrinsic property* of a given curve and that is why it is also referred to as a *geometric invariant*. Following [20, pp.203-204] it can be computed for any parametrization (I, F) of γ as :

$$\kappa(t) = \frac{\|\gamma'(t) \times \gamma''(t)\|}{\|\gamma'(t)\|^3} \quad , \quad \mathbf{t}'(t) = \|\gamma'(t)\|\kappa(t)\mathbf{n}(t) \quad (3.18)$$

Note that in eq. (3.17) the prime symbol denotes the derivative with respect to the natural parameter (s) while in eq. (3.18) it denotes the derivative with respect to any parameter (t). Consequently, the *speed* of the curve's parametrization appears in the latter equation :

$$v(t) = \frac{ds}{dt} = \|\gamma'(t)\| = s'(t) \quad (3.19)$$

The curvature measures how much a curve bends instantaneously in its osculating plane, that is how fast the tangent vector is rotating in the osculating plane around the binormal vector. In differential geometry this is expressed for a planar curve as :

$$\kappa(s) = \lim_{ds \rightarrow 0} \frac{\angle(\mathbf{t}(s), \mathbf{t}(s+ds))}{ds} = \lim_{ds \rightarrow 0} \frac{(\mathbf{t}(s+ds) - \mathbf{t}(s)) \cdot \mathbf{n}(s)}{ds} \quad (3.20)$$

where $\angle(\mathbf{t}(s), \mathbf{t}(s+ds))$ denotes the angle between $\mathbf{t}(s)$ and $\mathbf{t}(s+ds)$. This is equivalent as measuring how fast the osculating plane itself is rotating around the binormal vector. Consequently a curve is locally a *straight line* when its curvature vanishes ($\kappa(s) = 0$).

Radius of curvature

The *radius of curvature* is defined as the inverse of the curvature ($r = 1/\kappa$). From a geometric point of view, one can demonstrate that it is the radius of the osculating circle (see fig. 3.2). Remark that where the curvature vanishes the radius of curvature goes to infinity ; that is the osculating circle becomes a line, a circle of infinite radius.

Center of curvature

The *center of curvature* is defined as the center of the osculating circle (see fig. 3.2). The locus of all the centers of curvature of a curve is called the *evolute*.

Curvature binormal vector

Finally, following [21] we define the *curvature binormal vector*. Let γ be a biregular arc length parametrized curve. Let $s \in [0, L]$ be an arc length parameter. The *curvature binormal vector* is defined as :

$$\kappa \mathbf{b}(s) = \mathbf{t}(s) \times \mathbf{t}'(s) = \kappa(s) \cdot \mathbf{b}(s) \quad , \quad \|\kappa \mathbf{b}(s)\| = \kappa(s) \quad (3.21)$$

This vector will be useful as it embed all the necessary information on the curve's curvature. We will see in §3.5.6 that this vector is associated to the angular velocity of a specific adapted moving frame attached to the curve and called the *Bishop frame*.

3.4.2 Second invariant : the torsion

Let γ be a biregular arc length parametrized curve. Let $s \in [0, L]$ be an arc length parameter. The *torsion* is a scalar quantity defined as :

$$\tau_f(s) = \mathbf{n}'(s) \cdot \mathbf{b}(s) = -\mathbf{b}'(s) \cdot \mathbf{n}(s) \quad (3.22)$$

The torsion is *independent* regarding the choice of parametrization. This makes the torsion an *intrinsic property* of a given curve and that is why it is also referred to as a *geometric invariant*. Following [20, p.204] it can be computed for any parametrization (I, F) of γ as :

$$\tau_f(t) = \frac{\gamma'(t) \cdot (\gamma''(t) \times \gamma'''(t))}{\|\gamma'(t) \times \gamma''(t)\|^2} \quad \text{when} \quad \kappa(t) > 0 \quad (3.23)$$

The torsion measures how much a curve goes *instantaneously out of its plane*, that is to say how fast the normal or binormal vectors are rotating in the normal plane around the tangent vector. In differential geometry this is expressed as :

$$\tau_f(s) = \lim_{ds \rightarrow 0} \frac{\angle(\mathbf{n}(s), \mathbf{n}(s+ds))}{ds} = \lim_{ds \rightarrow 0} \frac{(\mathbf{n}(s+ds) - \mathbf{n}(s)) \cdot \mathbf{b}(s)}{ds} \quad (3.24)$$

This is equivalent as measuring how fast the osculating plane is rotating around the tangent vector. Consequently a curve is locally *plane* when its torsion vanishes ($\tau_f(s) = 0$).

Remark that the *torsion* is denoted “ τ_f ” and not simply “ τ ” as the latter will be reserved to denote any angular velocity of a moving adapted frame around its tangent vector. Thus, τ_f refers to the particular angular velocity of the Frenet trihedron around its tangent vector. This torsion, which is a geometric property of the curve, will be indifferently referred to as the *Frenet torsion* or the *geometric torsion*.

3.4.3 Fundamental theorem of space curves

This two *generalized curvatures*, respectively the curvature (κ) and the torsion (τ_f), are *invariant* regarding the choice of parametrization and under *euclidean motions*. The *Fundamental theorem of space curves* states that a curve is fully described, up to a

Euclidean motion of \mathbb{R}^3 , by its positive curvature ($\kappa > 0$) and torsion (τ_f) [20, p.229].

3.4.4 Serret-Frenet formulas

The *Fundamental theorem of space curves* is somehow a consequence of the *Serret-Frenet formulas*, which is the first-order system of differential equations satisfied by the Frenet trihedron. Let γ be a biregular arc length parametrized curve. Let $s \in [0, L]$ be an arc length parameter. Then, the Frenet trihedron satisfies the following formulas :

$$\mathbf{t}'(s) = \kappa(s)\mathbf{n}(s) \quad (3.25a)$$

$$\mathbf{n}'(s) = -\kappa(s)\mathbf{t}(s) + \tau_f(s)\mathbf{b}(s) \quad (3.25b)$$

$$\mathbf{b}'(s) = -\tau_f(s)\mathbf{n}(s) \quad (3.25c)$$

This system can be seen as the *equations of motion* of the Frenet trihedron moving along the curve γ at unit speed ($\|\gamma'\| = 1$). Indeed, introducing its *angular velocity vector* also known as the *Darboux vector* ($\mathbf{\Omega}_f$), the previous system is expressed as :

$$\begin{bmatrix} \mathbf{t}'(s) \\ \mathbf{n}'(s) \\ \mathbf{b}'(s) \end{bmatrix} = \mathbf{\Omega}_f(s) \times \begin{bmatrix} \mathbf{t}(s) \\ \mathbf{n}(s) \\ \mathbf{b}(s) \end{bmatrix} \quad \text{where} \quad \mathbf{\Omega}_f(s) = \begin{bmatrix} \tau_f(s) \\ 0 \\ \kappa(s) \end{bmatrix} \quad (3.26)$$

Because the Frenet trihedron satisfies a first-order system of differential equations of parameters κ and τ_f it is possible, by integration, to reconstruct the trace of the moving frame and thus the curve, up to a constant of integration (a trihedron in this case).

Finally, those formulas can be generalized to any non unit-speed parametrization of a curve.¹⁵ Let $\gamma = (I, F)$ be a biregular parametric curve. Let $t \in I$ be a parameter. Then the following *generalized Serret-Frenet formulas* hold :

$$\mathbf{t}'(t) = v(t)\kappa(t)\mathbf{n}(t) \quad (3.27a)$$

$$\mathbf{n}'(t) = -v(t)\kappa(t)\mathbf{t}(t) + v(t)\tau_f(s)\mathbf{b}(t) \quad (3.27b)$$

$$\mathbf{b}'(t) = -v(t)\tau_f(t)\mathbf{n}(t) \quad (3.27c)$$

Again, this system can be seen as the *equations of motion* of the Frenet trihedron moving along the curve γ at non unit-speed ($v(t) = \|\gamma'(t)\|$). This time the *angular velocity vector* ($\mathbf{\Omega}$) is distinct from the *Darboux vector* ($\mathbf{\Omega}_f$) and the previous system is expressed as :

$$\begin{bmatrix} \mathbf{t}'(t) \\ \mathbf{n}'(t) \\ \mathbf{b}'(t) \end{bmatrix} = \mathbf{\Omega}(t) \times \begin{bmatrix} \mathbf{t}(t) \\ \mathbf{n}(t) \\ \mathbf{b}(t) \end{bmatrix} \quad \text{where} \quad \mathbf{\Omega}(t) = v(t) \begin{bmatrix} \tau_f(t) \\ 0 \\ \kappa(t) \end{bmatrix} \quad (3.28)$$

¹⁵See [20, p.203] for a complete proof.

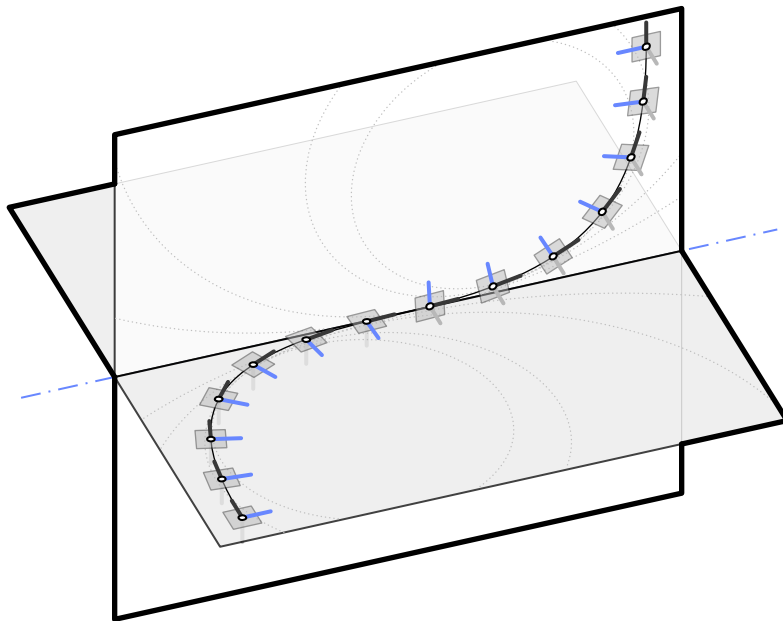


Figure 3.3 – Discontinuity of the Frenet trihedron at an inflexion point where the curvature vanishes and the orientation of the osculating plane is subject to a jump of angle $\pi/2$.

3.5 Curve framing

While the Frenet trihedron “has long been the standard vehicle for analysing properties of the curve invariant¹⁶ under euclidean motions” [5, p.1], a curve can be potentially framed with any arbitrary *moving frame*, understood as an *orthonormal basis field*. Thus, the Frenet frame is not the only way to frame a curve and other frames may also exhibit some interesting properties.¹⁷

In his paper [5] Bishop establishes the differential equation that a moving frame must satisfy and remarks that, because of the orthonormality condition, the first derivatives of the frame components can be expressed in terms of themselves through a skew-symmetric coefficient matrix. For such a frame, the understanding of its motion along the curve is thus reduced to the knowledge of only three scalar coefficient functions. He remarks that most of the interesting properties that the Frenet frame exhibits are due to the fact that one of these coefficient functions is vanishing everywhere on the curve (that is the frame is *rotation-minimizing* regarding one of its components) ; and that the Frenet frame is *adapted* to the curve (that is one of its components is nothing but the unit tangent vector).

In this section we introduce the notion of *moving frame* and two properties of interest that such a frame can exhibit in addition, namely : to be *adapted* to the curve ; and to be *rotation-minimizing* regarding a given direction. We then reconsider the case of the Frenet frame regarding this mathematical framework. Finally, we introduce the *zero-twisting* frame

¹⁶Namely the curvature (κ) and the Frenet torsion (τ_f).

¹⁷Recall the title of Bishop’s paper : “There is more than one way to frame a curve” [5].

also known as the *Bishop* frame.¹⁸ This tool will be fundamental for our futur study of slender beams.

3.5.1 Moving frame

Let γ be a curve parametrized by arc length. A map F which associates to each point of arc length parameter s a direct orthonormal trihedron is said to be a *moving frame* :

$$\begin{aligned} F : [0, L] &\longrightarrow \mathcal{SO}_3(\mathbb{R}) \\ s &\longmapsto F(s) = \{\mathbf{e}_3(s), \mathbf{e}_1(s), \mathbf{e}_2(s)\} \end{aligned} \quad (3.29)$$

Note that a direct orthonormal trihedron (or basis) is an element of the *rotation group* denoted \mathcal{SO}_3 . Consequently, a moving frame F attached to γ satisfies for all $s \in [0, L]$:

$$\|\mathbf{e}_i(s)\| = 1 \quad (3.30a)$$

$$\mathbf{e}_i(s) \cdot \mathbf{e}_j(s) = 0 \quad , \quad i \neq j \quad (3.30b)$$

The term “moving frame” will refer indifferently to the map itself (denoted $F = \{\mathbf{e}_3, \mathbf{e}_1, \mathbf{e}_2\}$), or to a specific evaluation of the map (denoted $F(s) = \{\mathbf{e}_3(s), \mathbf{e}_1(s), \mathbf{e}_2(s)\}$).

At first sight this indexing could seem strange but it will be convenient later in our mechanical model where \mathbf{e}_3 will be associated to the centerline’s tangent and \mathbf{e}_1 and \mathbf{e}_2 to the two cross-section principal axes of inertia. These axes will also be called *material axes*. We chose to introduce this indexing right now to maintain consistency between notations through out the chapters of this manuscript.

Governing equations

Computing the derivatives of the previous relationships leads to the following system of differential equations that the frame must satisfy for all $s \in [0, L]$:

$$\mathbf{e}'_i(s) \cdot \mathbf{e}_i(s) = 0 \quad (3.31a)$$

$$\mathbf{e}'_i(s) \cdot \mathbf{e}_j(s) = -\mathbf{e}_i(s) \cdot \mathbf{e}'_j(s) \quad , \quad i \neq j \quad (3.31b)$$

Thus, there exists 3 scalar functions (τ, k_1, k_2) such that $\{\mathbf{e}'_3, \mathbf{e}'_1, \mathbf{e}'_2\}$ can be expressed in the basis $\{\mathbf{e}_3, \mathbf{e}_1, \mathbf{e}_2\}$:

$$\mathbf{e}'_3(s) = k_2(s)\mathbf{e}_1(s) - k_1(s)\mathbf{e}_2(s) \quad (3.32a)$$

$$\mathbf{e}'_1(s) = -k_2(s)\mathbf{e}_3(s) + \tau(s)\mathbf{e}_2(s) \quad (3.32b)$$

$$\mathbf{e}'_2(s) = k_1(s)\mathbf{e}_3(s) - \tau(s)\mathbf{e}_1(s) \quad (3.32c)$$

¹⁸Named after Bishop who introduced it.

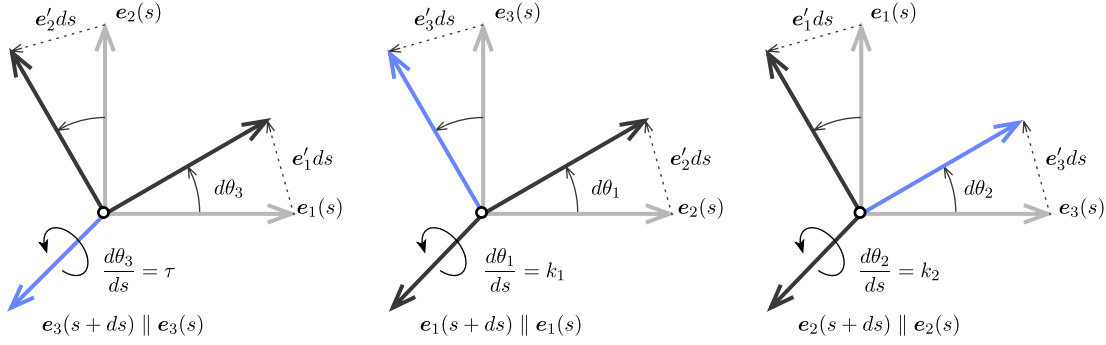


Figure 3.4 – Geometric interpretation of the angular velocity vector of a moving frame.

It is common to rewrite this first-order linear system of differential equations as a matrix equation : ^{19,20}

$$\begin{bmatrix} e'_3(s) \\ e'_1(s) \\ e'_2(s) \end{bmatrix} = \begin{bmatrix} 0 & k_2(s) & -k_1(s) \\ -k_2(s) & 0 & \tau(s) \\ k_1(s) & -\tau(s) & 0 \end{bmatrix} \begin{bmatrix} e_3(s) \\ e_1(s) \\ e_2(s) \end{bmatrix} \quad (3.33)$$

Since the progression of any moving frame along γ is ruled by a first-order system of differential equations, a unique triplet $\{\tau, k_1, k_2\}$ leads to a set of moving frames equal to each other within a constant of integration.²¹ Basically, with a given triplet $\{\tau, k_1, k_2\}$, one can propagate a given initial direct orthonormal trihedron (at $s = 0$ for instance) through the whole curve by integrating the system of differential equations. In general, a moving frame will be fully determined by τ , k_1 and k_2 together with the initial condition $\{e_3(s = 0), e_1(s = 0), e_2(s = 0)\}$.

Angular velocity

This system can be seen as the *equations of motion* of the frame moving along the curve γ at unit speed ($\|\gamma'\| = 1$). Indeed, introducing its *angular velocity vector* (Ω), the previous system is expressed as :

$$e'_i(s) = \Omega(s) \times e_i(s) \quad \text{avec} \quad \Omega(s) = \begin{bmatrix} \tau(s) \\ k_1(s) \\ k_2(s) \end{bmatrix} \quad (3.34)$$

This result is straightforward deduced from eq. (3.33). Note that the cross product reveals the skew-symmetric nature of the system, which could already be seen in eq. (3.33).

¹⁹In the case of a space curve, where e_3 is chosen to be the curve tangent unit vector and e_1 is chosen to be the curve normal unit vector, this set of equations is known as the *Serret-Frenet formulas*.

²⁰In the case of a space curve drawn on a surface, where e_3 is chosen to be the curve tangent unit vector and e_1 is chosen to be the surface normal unit vector, this set of equations is known as the *Darboux-Ribaucour formulas*.

²¹This assumption reminds the *Fundamental theorem of space curves* (§3.4.3).

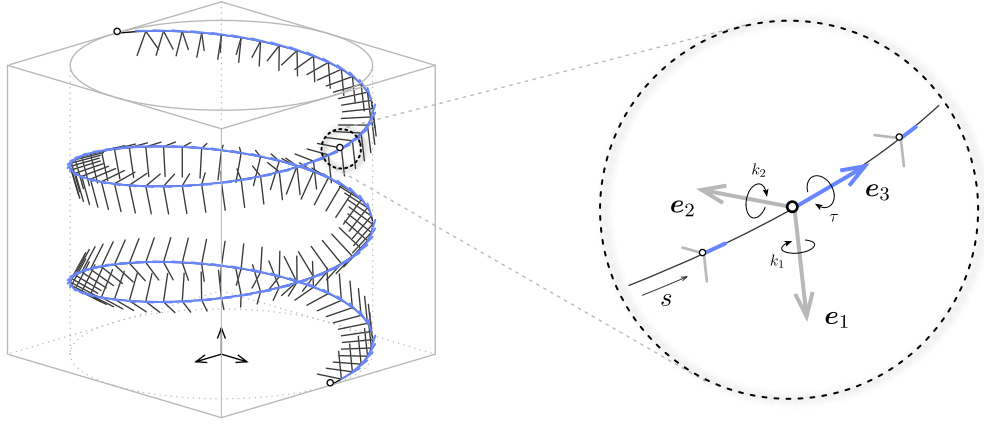


Figure 3.5 – Moving frame $F(s) = \{e_3(s), e_1(s), e_2(s)\}$ on a circular helix. The frame is adapted as $e_3(s) = t(s)$.

Geometrically, decomposing the infinitesimal rotation of the moving frame around its directors between arc length s and $s + ds$ (see fig. 3.4) shows that the scalar functions τ , k_1 and k_2 effectively correspond to the angular speed of the frame moving along γ , respectively around e_3 , e_1 and e_2 :

$$\frac{d\theta_3}{ds}(s) = \tau(s) \quad (3.35a)$$

$$\frac{d\theta_1}{ds}(s) = k_1(s) \quad (3.35b)$$

$$\frac{d\theta_2}{ds}(s) = k_2(s) \quad (3.35c)$$

3.5.2 Adapted moving frame

Let F be a moving frame as defined in the previous section. F is said to be *adapted* to γ if at each point $\gamma(s)$, $e_3(s)$ is the unit tangent vector of γ (fig. 3.5) :

$$e_3(s) = t(s) = \gamma'(s) \quad (3.36)$$

For an adapted frame, the components k_1 and k_2 of the angular velocity vector are related to the curvature of γ : ²²

$$\kappa(s) = \|e_3'(s)\| = \|k_2(s)e_1(s) + k_1(s)e_2(s)\| = \sqrt{k_1(s)^2 + k_2(s)^2} \quad (3.37)$$

²²This is why for an initially straight rod with an isotropic cross-section bending and torsion are uncoupled. Indeed, in that case the bending energy does not depend on the orientation of the cross-sections anymore as it depends only on the curvature of the rod : $\mathcal{E}_b = EI_1\kappa_1^2 + EI_2\kappa_2^2 = EI\kappa^2$.

Moreover, recalling the definition of the curvature binormal vector ($\kappa \mathbf{b}$) from eq. (3.21), it is easy to see that for an adapted moving frame the following relation holds :

$$\kappa \mathbf{b}(s) = k_1(s) \mathbf{e}_1(s) + k_2(s) \mathbf{e}_2(s) \quad (3.38)$$

Consequently, the angular velocity vector of an adapted moving frame can be written as :

$$\Omega(s) = \kappa \mathbf{b}(s) + \tau(s) \mathbf{t}(s) \quad (3.39)$$

This last result is very interesting as it shows that any adapted moving frame will differ from each other only by their twisting speed, as $\Omega_{\perp} = \kappa \mathbf{b}$ only depends on the curve.

3.5.3 Rotation-minimizing frame

Following [12, 11] we introduce the *rotation-minimizing frame* notion. A frame $\{\mathbf{e}_3, \mathbf{e}_1, \mathbf{e}_2\}$ is said to be *rotation-minimizing* regarding a given direction \mathbf{d} if :

$$\Omega(s) \cdot \mathbf{d}(s) = 0 \quad (3.40)$$

3.5.4 Parallel transport

The notion of *parallel transport* is somehow a generalization of the classical notion of collinearity in flat euclidean spaces (e.g. \mathbb{R}^2 or \mathbb{R}^3), to spaces that exhibit some non vanishing curvature (e.g. spheric or hyperbolic spaces).²³

Relatively parallel fields

Following Bishop 1975 [5], we define what is a (*relatively*) *parallel field*. Let γ be a regular curve parametrized by arc length. Let \mathbf{p} be a vector field along γ . The vector field \mathbf{p} is said to be *parallel* if its derivative is purely tangential, that is :

$$\mathbf{p}'(s) \times \mathbf{t}(s) = 0 \quad (3.41)$$

Consequently, for an adapted moving frame, the *normal fields* \mathbf{e}_1 and \mathbf{e}_2 are both *relatively parallels* if and only if the frame angular velocity is itself a normal field, that is :²⁴

$$\Omega(s) = \Omega_{\perp}(s) = \kappa \mathbf{b}(s) \Leftrightarrow \Omega(s) \cdot \mathbf{t}(s) = 0 \Leftrightarrow \tau(s) = 0 \quad (3.42)$$

In other words, a *relatively parallel normal field* : “turns, only whatever amount is necessary for it to remain normal, so it is as close to being parallel as possible without losing normality” [5].

²³<https://www.youtube.com/watch?v=p1tfZD2Bm0w>

²⁴A vector field \mathbf{p} is said to be *normal* along a curve γ if : $\forall s \in [0, L], \mathbf{p} \cdot \mathbf{t} = 0$.

Parallel transport of vectors along a curve

Reciprocally, it is possible to define the *parallel transport* of a vector along a curve γ as its propagation along γ at angular speed $\kappa \mathbf{b}$. An initial vector $\mathbf{p}_0 = \mathbf{p}(s_0)$ is parallel transported at arc length parameter s into the vector $\mathbf{p}(s)$ by integrating the following first-order differential equation along γ :

$$\mathbf{p}'(s) = \kappa \mathbf{b}(s) \times \mathbf{p}(s) \quad (3.43)$$

Consequently, the resulting vector field \mathbf{p} is a parallel field. Note that a parallel field is not necessarily a normal field.

From the point of view of differential geometry, this means that the next vector $\mathbf{p}(s + ds)$ is obtained by rotating the previous one $\mathbf{p}(s)$ around the curve binormal $\mathbf{b}(s)$ by an infinitesimal angle $d\theta(s) = \kappa(s)ds$. Note that $\mathbf{b}(s)$ has the same direction as $\mathbf{t}(s) \times \mathbf{t}(s + ds)$.

Parallel transport of frames along a curve

Identically, the *parallel transport* of an adapted frame is defined as the parallel transport of its components along γ .

3.5.5 Frenet frame

The Frenet frame is a well-known particular adapted moving frame. It is defined as the map that attach to any given point of γ the corresponding Frenet trihedron $\{\mathbf{t}(s), \mathbf{n}(s), \mathbf{b}(s)\}$ where :

$$\mathbf{t}(s) = \gamma'(s) \quad (3.44a)$$

$$\mathbf{n}(s) = \frac{\mathbf{t}'(s)}{\kappa(s)} \quad (3.44b)$$

$$\mathbf{b}(s) = \mathbf{t}(s) \times \mathbf{n}(s) \quad (3.44c)$$

Governing equations

The Frenet frame satisfies the *Frenet-Serret formulas* (see §3.4.4), which govern the evolution of the frame along the curve γ :

$$\begin{bmatrix} \mathbf{t}'(s) \\ \mathbf{n}'(s) \\ \mathbf{b}'(s) \end{bmatrix} = \begin{bmatrix} 0 & \kappa(s) & 0 \\ -\kappa(s) & 0 & \tau_f(s) \\ 0 & -\tau_f(s) & 0 \end{bmatrix} \begin{bmatrix} \mathbf{t}(s) \\ \mathbf{n}(s) \\ \mathbf{b}(s) \end{bmatrix} \quad (3.45)$$

Remember the generic system of differential equations of an adapted moving frame attached to a curve, established in eq. (3.33), where $\mathbf{e}_3(s) = \mathbf{t}(s)$, $k_1(s) = 0$, $k_2(s) = \kappa(s)$ and $\tau(s) = \tau_f(s)$.

Angular velocity

Consequently, the angular velocity vector ($\boldsymbol{\Omega}_f$) of the Frenet frame, also known as the *Darboux vector* in this particular case, is given by :

$$\boldsymbol{\Omega}_f(s) = \begin{bmatrix} \tau_f(s) \\ 0 \\ \kappa(s) \end{bmatrix} = \kappa \mathbf{b}(s) + \tau_f(s) \mathbf{t}(s) \quad (3.46)$$

Remark that the Frenet frame satisfies $\boldsymbol{\Omega}_f(s) \cdot \mathbf{n}(s) = 0$ and is thus a *rotation-minimizing* frame regarding the normal vector (\mathbf{n}). The motion of this frame through the curve is known as *pitch-free*.

Note also that $\mathbf{t}'(s)$ and $\mathbf{b}'(s)$ are collinear to $\mathbf{n}(s)$. This means that the projection of $\mathbf{t}(s)$ and $\mathbf{b}(s)$ is conserved from one normal plane to another, that is \mathbf{t} and \mathbf{b} are parallel transported along the vector field \mathbf{n} .

Drawbacks and benefits

The Frenet frame is not continuously defined if γ is not \mathcal{C}^2 . This is problematic for the study of slender beams as the centerline of a beam subject to punctual external forces and moments or to material discontinuities will not be \mathcal{C}^2 but only piecewise \mathcal{C}^2 . In that case, the centerline tangent will be continuously defined everywhere but the curvature will be subject to discontinuities, that is \mathbf{t}' will not be continuously defined.

Moreover, even if γ is \mathcal{C}^2 , the Frenet frame is not defined where the curvature vanishes, which obviously is an admissible configuration for a beam centerline. This issue can be partially addressed by parallel transporting the normal vector along the straight regions of the curve. Thus, the extended frame will still satisfy the governing equations exposed in [eq. \(3.45\)](#). However, if the osculating planes are not parallels on both sides of a region of null curvature, torsion will be subject to a discontinuity and so the Frenet frame ([fig. 3.3](#)).²⁵ Again, if the region of null curvature is not a point, that is the region is not an inflexion point but a locus where the curve is locally a straight line, the change in torsion on both sides of the region can be accommodated by a continuous rotation from one end to the other.

One benefit of the Frenet frame is that, when transported along a *closed curve*, the frame at the end of the curve will align back with the frame at the beginning of the curve, that is the frame will returns to its initial value after a complete turn. During its trip, the frame will make a total twist of $\int_0^L \tau_f(s) ds = 0[2\pi]$ around the tangent vector.

A second benefit is that any adapted frame can be obtained by a rotation of the Frenet frame around the unit tangent vector [7, p.2].

²⁵This is also highlighted in [8, 11].

3.5.6 Bishop frame

A *Bishop frame* denoted $\{\mathbf{t}, \mathbf{u}, \mathbf{v}\}$, also known as *zero-twisting* or *parallel-transported* frame, is an adapted moving frame that has no tangential angular velocity : ²⁶

$$\boldsymbol{\Omega} \cdot \mathbf{t} = \tau = \mathbf{u}' \cdot \mathbf{v} = -\mathbf{u} \cdot \mathbf{v}' = 0 \quad (3.47)$$

Because a Bishop frame is an adapted frame, it can be defined relatively to the Frenet frame by a rotation around the unit tangent vector. A Bishop frame is a frame that cancels out the rotational movement of the Frenet frame around the tangent vector. At arc length parameter s , the Frenet frame has continuously rotated around its tangent vector of a cumulative angle : $\int_0^s \tau_f(t) dt$. Thus, any Bishop frame will be obtained, within a constant rotation angle θ_0 , through a rotation of the Frenet frame around the tangent vector by an angle :

$$\theta(s) = - \int_0^s \tau_f(t) dt + \theta_0(s) \quad (3.48)$$

Consequently, a Bishop frame can be expressed relatively to the Frenet frame as :

$$\begin{cases} \mathbf{u} = \cos \theta \mathbf{n} + \sin \theta \mathbf{b} \\ \mathbf{v} = -\sin \theta \mathbf{n} + \cos \theta \mathbf{b} \end{cases} \quad (3.49)$$

Governing equations

The Bishop frame satisfies the following system of differential equations, which governs the evolution of the frame along the curve γ :

$$\begin{bmatrix} \mathbf{t}'(s) \\ \mathbf{u}'(s) \\ \mathbf{v}'(s) \end{bmatrix} = \begin{bmatrix} 0 & \kappa(s) \sin \theta(s) & -\kappa(s) \cos \theta(s) \\ -\kappa(s) \sin \theta(s) & 0 & 0 \\ \kappa(s) \cos \theta(s) & 0 & 0 \end{bmatrix} \begin{bmatrix} \mathbf{t}(s) \\ \mathbf{u}(s) \\ \mathbf{v}(s) \end{bmatrix} \quad (3.50)$$

One can remember the generic differential equations of an adapted moving frame attached to a curve, where : ²⁷

$$k_1(s) = \kappa(s) \sin \theta(s) \quad , \quad k_2(s) = \kappa(s) \cos \theta(s) \quad , \quad \tau(s) = 0 \quad (3.51)$$

²⁶Bishop frames were introduced as *relatively parallel adapted frames* in [5].

²⁷

$$\tau = \mathbf{u}' \cdot \mathbf{v} = (\boldsymbol{\Omega}_f \times \mathbf{u} + \theta' \mathbf{v}) \cdot \mathbf{v} = \tau_f - \tau_f = 0$$

$$k_1 = -\mathbf{t}' \cdot \mathbf{v} = -\kappa \mathbf{n} \cdot \mathbf{v} = \kappa \sin \theta$$

$$k_2 = \mathbf{t}' \cdot \mathbf{u} = \kappa \mathbf{n} \cdot \mathbf{u} = \kappa \cos \theta$$

Angular velocity

Consequently, the angular velocity vector ($\mathbf{\Omega}_b$) of the Bishop frame is given by :

$$\mathbf{\Omega}_b(s) = \begin{bmatrix} 0 \\ \kappa(s) \sin \theta(s) \\ \kappa(s) \cos \theta(s) \end{bmatrix} = \kappa \mathbf{b}(s) \quad (3.52)$$

Remark that the Bishop frame satisfies $\mathbf{\Omega}_b(s) \cdot \mathbf{t}(s) = 0$ and is thus *rotation-minimizing* regarding the tangent vector. The motion of this frame through the curve is known as “roll-free”.

Because the motion of this frame is described by an angular velocity vector that is nothing but the curvature binormal vector ($\mathbf{\Omega}_b = \kappa \mathbf{b}$), it can be interpreted in terms of *parallel transport* as defined in §3.5.4. Thus, given an initial frame at arc length parameter $s = 0$, the Bishop frame at any arc length parameter (s) is obtained by parallel transporting the initial frame $\{\mathbf{t}(0), \mathbf{u}(0), \mathbf{v}(0)\}$ along the curve from 0 to s .

Drawbacks and benefits

One of the main benefits of the Bishop frame is that its generative method : “is immune to degeneracies in the curvature vector” [8]. Although we first expressed the construction of the Bishop frame relatively to the Frenet frame (which exists wherever γ is biregular), the existence of the Bishop frame, understood in terms of parallel transport, is guaranteed wherever the curvature binormal ($\kappa \mathbf{b} = \mathbf{t} \times \mathbf{t}'$) is defined. To be continuously defined over $[0, L]$, a Bishop frame only needs the curvature binormal vector to be piecewise continuously defined over $[0, L]$, which only requires that γ' is \mathcal{C}^0 and that γ'' is piecewise \mathcal{C}^0 . Obviously, those weaker existence conditions are profitables to bypass the drawbacks of the Frenet frame regarding the modeling of slender beams listed in §3.5.5.

Strictly speaking, a Bishop frame is not a reference frame as it is defined within an initial condition. However, we will see later that strains in a beam are modeled as a rate of change in the Bishop frame, and consequently the initial condition will disappear in the equations.

Unlike the Frenet frame, when transported along a *closed curve*, the Bishop frame at the end of the curve will not necessarily align back with the frame at the beginning of the curve.²⁸ Even if the frame returns to its initial value after a complete turn, it may returns in its position after several complete turns ($2k\pi$) around the curve tangent. During its movement along the curve, the frame will make a total twist of $\int_0^L \tau_f(s) ds = \alpha[2\pi]$ around the tangent vector. This difference of angle is related to the concept of *holonomy*.

Remark also that Frenet and Bishop frames coincide for planar curves ($\tau_f = 0$), within a constant rotation around the unit tangent vector.

²⁸“it is possible for closed curves to have parallel transport frames that do not match up after one full circuit of the curve” [9].

3.5.7 Comparison between Frenet and Bishop frames

Let γ be a *circular helix* of parameter a and k . In a cartesian coordinate system, it is defined as :

$$\mathbf{r}(t) = [a \cos t, a \sin t, kt] = a \cos t \mathbf{e}_x + a \sin t \mathbf{e}_y + kt \mathbf{e}_z \quad (3.53)$$

The speed of this parametrization, the curvature and the geometric torsion are uniform and given by :

$$v(t) = \sqrt{a^2 + k^2} \quad (3.54a)$$

$$\kappa(t) = \frac{a}{a^2 + k^2} \quad (3.54b)$$

$$\tau_f(t) = \frac{k}{a^2 + k^2} \quad (3.54c)$$

The Frenet frame components are given by (with $\alpha = v\kappa$ and $\beta = v\tau_f$) :

$$\mathbf{t}(t) = [-\alpha \cos t, \alpha \sin t, \beta t] \quad (3.55a)$$

$$\mathbf{n}(t) = [-\cos t, -\sin t, 0] \quad (3.55b)$$

$$\mathbf{b}(t) = [\beta \sin t, -\beta \cos t, \alpha] \quad (3.55c)$$

And the Bishop frame components are given by :

$$\mathbf{u}(t) = [-\cos t \cos \beta t - \beta \sin t \sin \beta t, -\sin t \cos \beta t + \beta \cos t \sin \beta t, -\alpha \sin \beta t] \quad (3.56a)$$

$$\mathbf{v}(t) = [-\cos t \sin \beta t + \beta \sin t \cos \beta t, -\sin t \sin \beta t - \beta \cos t \cos \beta t, \alpha \cos \beta t] \quad (3.56b)$$

At $t = 0$ the two frames coincide. At $t > 0$ the Bishop frame is obtained from the Frenet frame by a rotation around $\mathbf{t}(t)$ of an angle $\theta(t) = -\tau_f \cdot (vt)$.

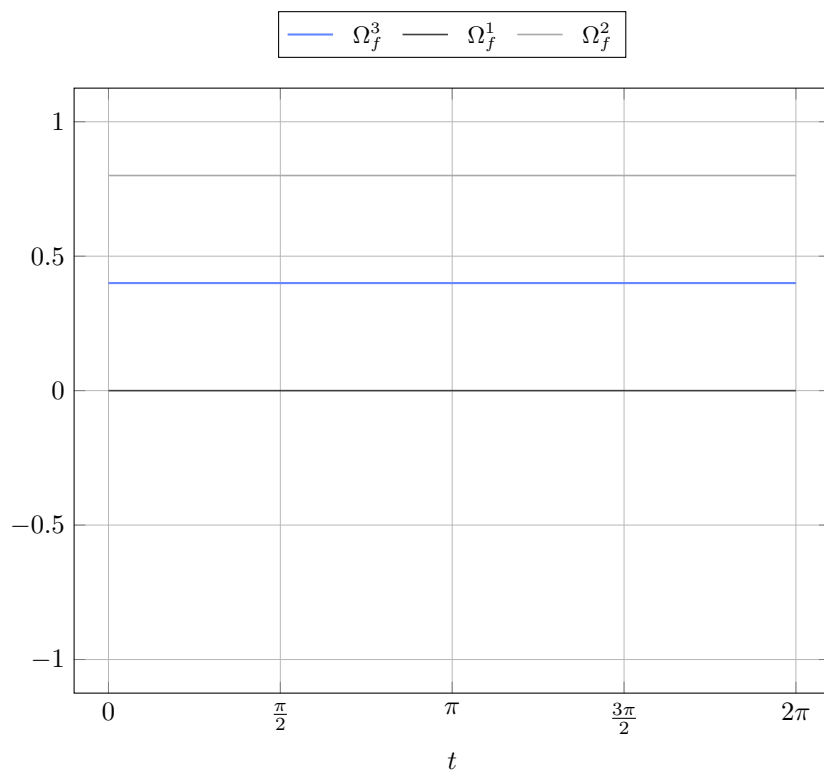
The angular velocities of the Frenet and Bishop frames are respectively given by :

$$\mathbf{\Omega}_f(t) = [\tau_f, 0, \kappa] \quad (3.57a)$$

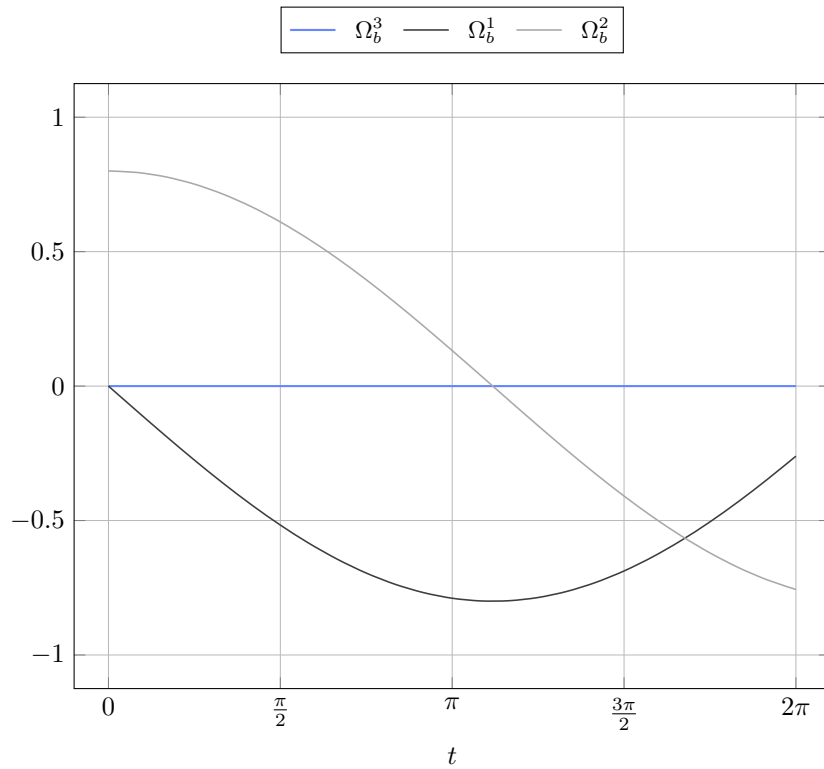
$$\mathbf{\Omega}_b(t) = [0, \kappa \sin \theta, \kappa \cos \theta] \quad (3.57b)$$

The components of these angular velocities are plotted in [fig. 3.6](#) for a circular helix with parameter $a = 1.0$ and $k = 0.5$ while the parameter t varies from 0 to 2π . At $t = 2\pi$ the frame has made a full turn and its altitude has increased from 0 to π .

The components of the angular velocity of the Frenet frame are constant during the movement along the curve and the frame does not rotate around the normal vector as $\Omega_f^2 = 0$ (see [fig. 3.6a](#)). The components of the angular velocity of the Bishop frame vary during the movement along the curve and the frame does not rotate around the tangent vector as $\Omega_b^3 = 0$ (see [fig. 3.6b](#)).



(a) Frenet frame



(b) Bishop frame

Figure 3.6 – Angular velocities of Frenet and Bishop frames for a circular helix ($a = 1.0$ and $k = 0.5$).

3.6 Discrete curves

The previous section has introduced the fundamental analytical tools to develop a solid understanding of the geometry of smooth space curves. These tools will be essentials for the construction of the beam model presented later in ?? and ?. In this section we look for equivalent notions in the case of discrete space curves, as the developed model will be implemented in a numerical program to solve real mechanical problems through discrete element models (see ?).

The study of those discrete equivalent notions belong to the recent field of *Discrete Differential Geometry* : “In some sense discrete differential geometry can be considered more fundamental than differential geometry since the later can be obtained from the former as a limit” [3, p.7]. In particular, we will see that there are several ways to define the discrete equivalents of the curvature and the unit tangent vector. Though these various ways are equivalent and match their smooth counterpart by passing to the limit, they exhibit different capabilities at the discrete level.

“There is no general theory or methodology in the literature, despite the ubiquitous use of discrete curves in mathematics and science. There are conflicting definitions of even basic concepts such as discrete curvature κ , discrete torsion τ , or discrete Frenet frame.” [22, p.1].

3.6.1 Definition

Let Γ be a discrete (or polygonal) space curve. Γ is defined as an ordered sequence $\Gamma = (\mathbf{x}_0, \mathbf{x}_1, \dots, \mathbf{x}_n) \in \mathbb{R}^{3(n+1)}$ of $n + 1$ pairwise disjoint *vertices* (see fig. 3.7). Consecutive pairs of vertices define n straight segments $(\mathbf{e}_0, \mathbf{e}_1, \dots, \mathbf{e}_{n-1})$ called *edges*, pointing from one vertex to the next one : $\mathbf{e}_i = \mathbf{x}_{i+1} - \mathbf{x}_i$. The midpoint of \mathbf{e}_i is a vertex denoted : $\mathbf{x}_{i+1/2} = \mathbf{x}_i + \frac{1}{2}\mathbf{e}_i$.

The length of \mathbf{e}_i is denoted $l_i = \|\mathbf{e}_i\|$. The total length of Γ is denoted $L = \sum_{i=0}^{n-1} \|\mathbf{e}_i\|$. Additionally, we define the vertex-based mean length \bar{l}_i at vertex \mathbf{x}_i :

$$\begin{cases} \bar{l}_0 = l_0 & i = 0 \\ \bar{l}_i = \frac{1}{2}(l_{i-1} + l_i) & i \in \llbracket 1, n-1 \rrbracket \\ \bar{l}_n = l_{n-1} & i = n \end{cases} \quad (3.58)$$

Discrete unit tangent vector

Edge vectors lead to a natural definition of the *discrete unit tangent vector* along each edge : $\mathbf{u}_i = \mathbf{e}_i / l_i$. However, this definition makes no sense at vertices where all the curvature is condensed and measured by the turning angle (φ_i) . This is often illustrated in terms of the Gauß map, a transformation in which edges will map to points and vertices will map to

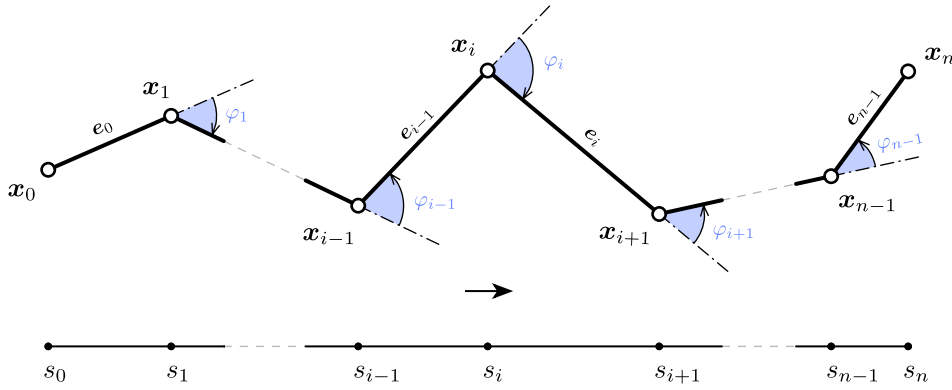


Figure 3.7 – Discrete curve representation and parametrization.

curves on the unit sphere.

Discrete osculating plane

Consecutive pairs of edges lead to a natural definition of the *discrete osculating plane*, as the plane in which Γ locally lies on. This plane is well defined by its normal vector known as the *discrete unit binormal vector* ($\mathbf{b}_i = \frac{\mathbf{e}_{i-1} \times \mathbf{e}_i}{\|\mathbf{e}_{i-1} \times \mathbf{e}_i\|}$) only if \mathbf{e}_{i-1} and \mathbf{e}_i are non-collinear ; that is the curve is not locally a straight line, or equivalently the curvature does not vanish.

Discrete turning angle

The *turning angle* is defined as the oriented angle between to adjacent edges : $\varphi_i = \angle(\mathbf{e}_{i-1}, \mathbf{e}_i)$. It is defined only for all $i \in \llbracket 1, n-1 \rrbracket$. It corresponds to the angle of rotation, in the osculating plane, around the binormal vector (\mathbf{b}_i), to align \mathbf{e}_{i-1} with \mathbf{e}_i . The sign of φ_i is taken in accordance to the right-hand rule regarding the orientation of \mathbf{b}_i . Thus, φ_i is necessarily bounded to $[0, \pi]$:

$$0 \leq \varphi_i \leq \pi \quad (3.59)$$

The next section will highlight the central role of the turning angle in the possible measurements of the discrete curvature.

Recall that for a planar curve, where φ denotes the angle between the tangent vector ($\mathbf{t} = \cos \varphi \mathbf{e}_x + \sin \varphi \mathbf{e}_y$) and the horizontal line of direction \mathbf{e}_x , the following relation holds : $\varphi(s_1) - \varphi(s_2) = \int_{s_1}^{s_2} \frac{d\varphi}{ds} ds = \int_{s_1}^{s_2} \kappa ds$.

3.6.2 Regularity

Let $\Gamma = (x_0, x_1, \dots, x_n)$ be a discrete curve of edges $\mathbf{e}_0, \mathbf{e}_1, \dots, \mathbf{e}_{n-1}$. Γ is said to be :

- *regular* if it has no kinks : $\mathbf{e}_{i-1} + \mathbf{e}_i \neq 0 \Leftrightarrow \varphi_i \neq \pi \mid \forall i \in \llbracket 1, n-1 \rrbracket$

- *biregular* if no vertex is flat : $\mathbf{e}_{i-1} - \mathbf{e}_i \neq 0 \Leftrightarrow \varphi_i \neq 0 \mid \forall i \in \llbracket 1, n-1 \rrbracket$

3.6.3 Parametrization

In the literature, discrete curves are usually considered as maps defined on $I = \llbracket 0, n \rrbracket \in \mathbb{N}^{n+1}$. As a consequence, the discrete derivative of Γ is an edge-based quantity defined as :

$$\Gamma'_i = \frac{\Gamma(t_{i+1}) - \Gamma(t_i)}{t_{i+1} - t_i} = \mathbf{e}_i \quad , \quad \mathbf{x}_i = \Gamma(t_i) \quad , \quad t_i = i \quad (3.60)$$

Thus, as in the smooth case, a discrete curve is said to be parametrized by arc length if $\|\Gamma'\| = 1$, that is every edges are of unit length ($\|\mathbf{e}_i\| = 1$).²⁹ This constraint is sometimes relaxed to curves of constant edge length ($\|\mathbf{e}_i\| = c$) that are said to be parametrized *proportional* to arc length.

In the present work, to stick closer to the smooth case, we instead consider discrete curves as maps defined on $I = [t_0, t_1, \dots, t_n] \in \mathbb{R}^{n+1}$ where t denotes the discrete parametrization of Γ . As in the smooth case, the way to parametrized a curve is not unique.

Arc length parameter

By analogy with the smooth case, we define the curve arc length at vertices (see [fig. 3.7](#)) as :

$$\begin{cases} s_0 = 0 & i = 0 \\ s_i = \sum_{k=1}^i \|\mathbf{e}_{k-1}\| & i \in \llbracket 1, n-1 \rrbracket \\ s_n = L & i = n \end{cases} \quad (3.61)$$

This definition naturally extends to the whole domain by piecewise linear interpolation. This is not different as considering the discrete curve as a continuous polygonal curve. Indeed, for any $s \in [s_i, s_{i+1}]$ there exists a normalized parameter $t = \frac{s-s_i}{s_{i+1}-s_i} \in [0, 1]$ so that :

$$s(t) = (1-t)s_i + ts_{i+1} = s_i + tl_i \quad (3.62a)$$

$$\mathbf{x}(t) = (1-t)\mathbf{x}_i + t\mathbf{x}_{i+1} = \mathbf{x}_i + t\mathbf{e}_i \quad (3.62b)$$

Note that this parametrization satisfies $\|\Gamma'\| = 1$ on $\bigcup_{i=1}^n]s_{i-1}, s_i[$ but Γ' remains undefined at vertices. This issue is the reason why defining the tangent vector at vertices can not be done unequivocally for discrete curves.

²⁹This assumption leads to the assertion that “A discrete curve is parameterized by arc length or it is not” [3, p.10].

3.7 Discrete curvature

Vouga 2014 [4] defines and compares three different definitions of the discrete curvature that does not suppose that $\|e_i\|$ is constant. By trying to mimic some properties of the curvature in the smooth case Carroll et al. 2014 [22] and Bobenko 2015 [23] also define and compare three different definitions of the discrete curvature from the osculating circle. One main drawback of all the said proposals is that the question of the curvature at start and end points is never treated. But this is of main importance when dealing with beams as the nature of the boundary conditions can make the curvature to be null or not at its ends, depending if somme moment has to be transfer or not. In this sens, the question of discrete curvature could not be treated separately with the question of the tangent vector.

3.7.1 Definition from osculating circles

Curvature is defined from the osculating circle, which is the best approximation of a curve by a circle.

Vertex-based osculating circle (circumscribed)

Let Γ be a discrete curve parametrized by arc length. The *vertex-based* (or circumscribed) osculating circle at vertex x_i is defined as the unique circle passing through the points x_{i-1} , x_i and x_{i+1} (see fig. 3.8a). This circle leads to the following definition of the curvature : ³⁰

$$\kappa b_i = \frac{2 e_{i-1} \times e_i}{\|e_{i-1}\| \|e_i\| \|e_{i-1} + e_i\|} \quad , \quad \kappa_i = \|\kappa b_i\| = \frac{2 \sin(\varphi_i)}{\|e_{i-1} + e_i\|} \quad (3.63)$$

This definition shows a good locality as the curvature is attached to the vertex x_i , right in the place where it occurs on the discret curve. In addition, this definition leads to a natural local spline interpolation by the circumscribed osculating circle itself. This interpolation has the advantage to pass exactly through three vertices, to lie on the osculating plane and to share the same curvature as Γ at x_i . It also leads to a natural definition of the tangent vector at x_i (see ??).

Moreover, while this definition is valid only on the current portion of Γ ($i \in [1, n-1]$), it is straightforward extended to its endings ($i = 0, 1$), provided that a unit tangent vector t_0 (respectively t_n) is given at x_0 (resp. x_n), as the unique circle tangent to t_0 (resp. t_n) passing through x_0 and x_1 (resp. x_{n-1} and x_n) :

$$\kappa b_0 = \frac{2 e_0 \times t_0}{\|e_0\|^2} \quad , \quad \kappa b_n = \frac{2 t_n \times e_{n-1}}{\|e_{n-1}\|^2} \quad (3.64)$$

This property will be very profitable in the discrete beam model developed later in the manuscript. It is examined more in details in section ?? about the definition of the tangent vector.

³⁰This curvature is also known as the *Menger curvature*.

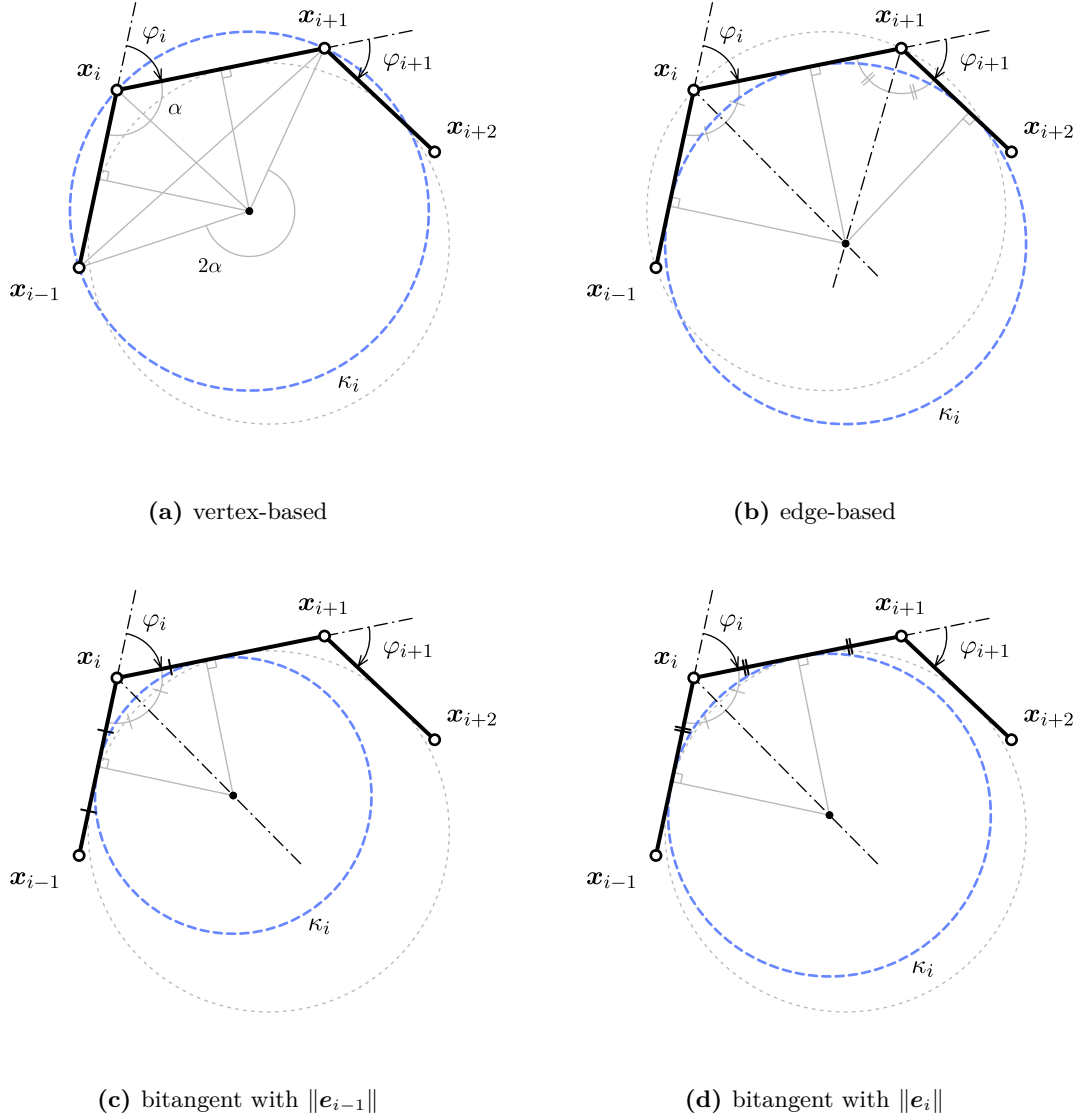


Figure 3.8 – Several ways to define the osculating circle for discrete curves, leading to different notions of discrete curvature.

Curvature (κ_i)	Locality	$\varphi \mapsto 0$	$\varphi \mapsto \pi$	Ends	Dim	Fitting
$\kappa_1 = \frac{2 \sin(\varphi_i)}{\ e_{i-1} + e_i\ }$	x_i	0	0, 2	yes	space	clothoid
$\kappa_2 = \frac{\tan(\varphi_i/2) + \tan(\varphi_{i+1}/2)}{l_i}$	e_i	0	∞	no	planar	circle
$\kappa_3 = \frac{2 \tan(\varphi_i/2)}{l_i}$	x_i	0	∞	no	space	circles
$\kappa_4 = \frac{2 \sin(\varphi_i/2)}{l_i}$	x_i	0	0, 2	no	space	clothoid
$\kappa_5 = \frac{\varphi_i}{l_i}$	x_i	0	π/\bar{l}_i	no	space	elastica

Table 3.1 – Review of several discrete curvature definitions mentioned in the literature.

However, there are some important drawbacks as the curvature is bounded to $[0, 2]$ (see [fig. 3.10](#)). When the curve tends to kinks ($\varphi \mapsto \pi$), one would expect the curvature to diverge toward infinity, but instead it tends to a finite value equals to 0 ($l_{i-1} \neq l_i$) or 2 ($l_{i-1} = l_i$). This issue can be bypassed if the discretization is refined “enough”. A criterion is given in the next section ([§3.7.2](#)).

Edge-based osculating circle (inscribed)

Let Γ be a discrete curve parametrized by arc length. The *edge-based* osculating circle at edge \mathbf{e}_i is defined as the unique circle tangent to the edges \mathbf{e}_{i-1} , \mathbf{e}_i and \mathbf{e}_{i+1} (see [fig. 3.8b](#)).

$$\kappa_i = \frac{\tan(\varphi_i/2) + \tan(\varphi_{i+1}/2)}{\|\mathbf{e}_i\|} \quad (3.65)$$

This definition shows an appropriate behavior : when the curve tends to kinks the radius of curvature tends to zero ($\tan \varphi/2 \mapsto \infty$), and when the curve tends to be a straight line the curvature tends to 0 ($\tan \varphi/2 \mapsto 0$).

However, it needs Γ to be planar which is by far too restrictive regarding our goal (the modeling of 3D slender beams). Finally, this way of defining the curvature is not as local as one would expect as it is defined relatively to the edge \mathbf{e}_i but not where the turning occurs, at vertices.

Bitangent osculating circle (inscribed)

Let Γ be a discrete curve parametrized by arc length. Following [\[4\]](#) we define the curvature regarding the mean length \bar{l}_i attached to \mathbf{x}_i as : ³¹

$$\kappa \mathbf{b}_i = \frac{2}{\bar{l}_i} \left(\frac{\mathbf{e}_{i-1} \times \mathbf{e}_i}{\|\mathbf{e}_{i-1}\| \|\mathbf{e}_i\| + \mathbf{e}_{i-1} \cdot \mathbf{e}_i} \right) \quad , \quad \kappa_i = \|\kappa \mathbf{b}_i\| = \frac{2}{\bar{l}_i} \tan(\varphi_i/2) \quad (3.66)$$

This other definition combines the good locality of the vertex-based approach (see [eq. \(3.63\)](#)) and the proper behavior at bounds of the edge-based approach (see [eq. \(3.65\)](#)). Given two adjacent edges \mathbf{e}_{i-1} and \mathbf{e}_i , there exists an infinite number of circles that are tangent to both edges (see [fig. 3.8c](#) and [fig. 3.8d](#) for two remarkable circles among them), which center points all lie on the $\varphi_i - \pi$ angle bisector line. The corresponding osculating circle, known as the *inscribed* circle, is constructed to touch both \mathbf{e}_{i-1} and \mathbf{e}_i at distance \bar{l}_i from \mathbf{x}_i . In the case of a constant edge length discrete curve, this definition of the osculating circle merges to the circles proposed in [fig. 3.8c](#) and [fig. 3.8d](#).

However, this definition still exhibits some drawbacks. Firstly, remark that there is an infinity of possible inscribed circles (defined as a circle that is bitangent to two connected edges). Indeed, this circle is unique only if the distance between the common vertex and the points of tangency are prescribed. Although it could seem natural to take the middle

³¹This definition is also presented in [\[23, 22\]](#) but in the more restrictive case of constant edge length discrete curves ($l_i = cst$).

of the edges as points of tangency if they have the same length ($\|\mathbf{e}_i\| = \|\mathbf{e}_{i+1}\|$), there is no obvious choice at all for this parameter (compare [fig. 3.8c](#) with [fig. 3.8d](#)). Moreover, the lack of a natural interpolation spline that passes through the vertices and that is in correlation to the osculating circle is also detrimental in the context of our application.

Other definitions of osculating circles

In the literature, one can find other definitions for the discrete curvature that also correspond to the definition of an osculating circle. All these definitions are summarized in [tab. 3.1](#). For further informations, the reader should refer to [\[22, 4, 23, 24\]](#).

In particular, Vouga [\[4\]](#) details which discrete curvature definitions parallel which property of the smooth curvature. He remarks that there is no “free-lunch” as none of the proposed definition satisfies every properties of the smooth curvature.

3.7.2 Benchmarking : sensitivity to non uniform discretization

In this section we compare the two main discrete curvature notions (circumscribed versus inscribed) regarding their sensibility to non uniform discretization.

This aspect is not treated in the actual literature, in which curves parametrized by arc length are usually treated as curves of constant edge length, though it is yet an important topic when it comes to the numerical modeling of true mechanical systems. Indeed, the presence of connexions between members will compromise the ability to enforce a constant discretization through all the elements of the structure. Additionally, vertices are obviously points of interest in a discrete model as they will be used to apply loads and enforce various constraints such as joints and support conditions. Finally, the accuracy of the discretized model is proportional to the sharpness of the discretization, whereas the computing time required to solve the model will grow as the sharpness increases. Consequently, one would distribute those points in the space as cleverly as possible and try to minimize their number as they increase the overall computation cost.

Introducing the coefficient $\alpha = \frac{\|\mathbf{e}_{i-1}\|}{\|\mathbf{e}_i\|}$, we rewrite the previous formulas for κ_1 and κ_3 as :

$$\begin{aligned}\kappa_1 &= \frac{2 \sin(\varphi)}{\|\mathbf{e}_i\|(1 + \alpha^2 + 2\alpha \cos(\varphi))^{1/2}} \\ \kappa_3 &= \frac{4 \tan(\varphi/2)}{\|\mathbf{e}_i\|(1 + \alpha)}\end{aligned}\tag{3.67}$$

These expressions lead to the following formula for the ratio κ_1/κ_3 , which relies only on α and the turning angle φ between the edges \mathbf{e}_{i-1} and \mathbf{e}_i :

$$\frac{\kappa_1}{\kappa_3}(\alpha) = \frac{\kappa_1}{\kappa_3}(1/\alpha) = \frac{(1 + \alpha) \cos^2(\varphi/2)}{((1 - \alpha)^2 + 4\alpha \cos^2(\varphi/2))^{1/2}}\tag{3.68}$$

Discrete curvatures are plotted in [fig. 3.10](#) for three values of α . The thickest line is for the

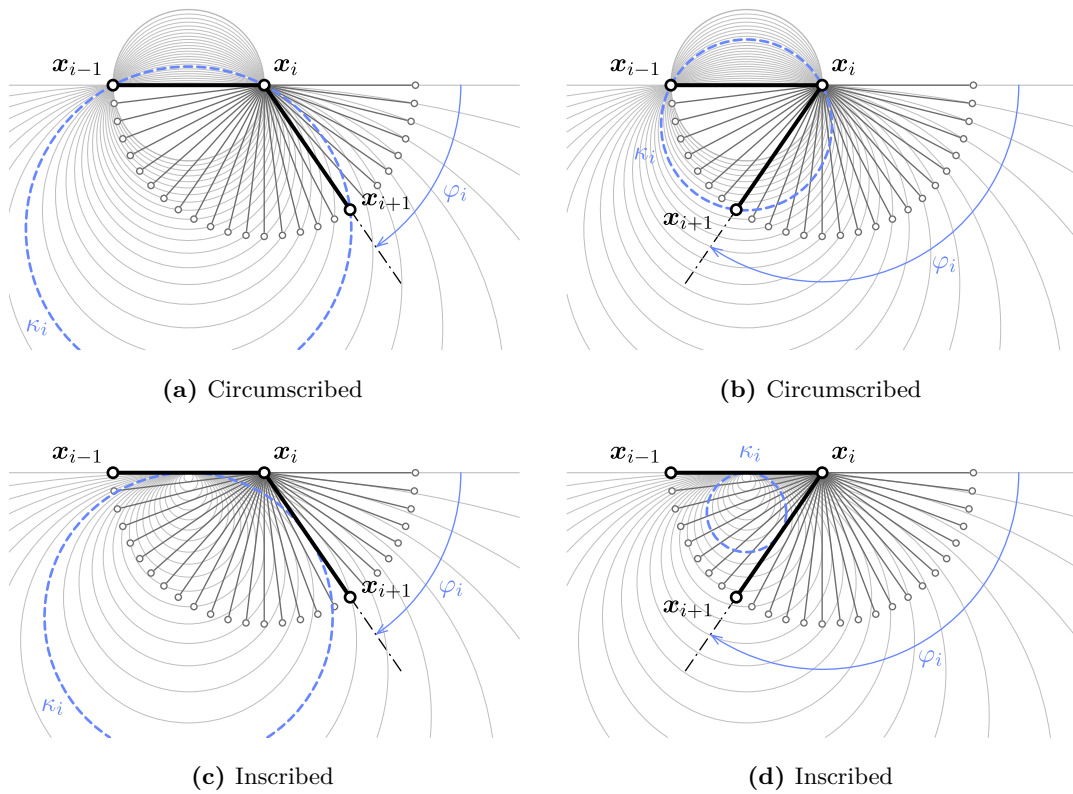


Figure 3.9 – Comparison of circumscribed and inscribed osculating circles for different values of the turning angle (φ).

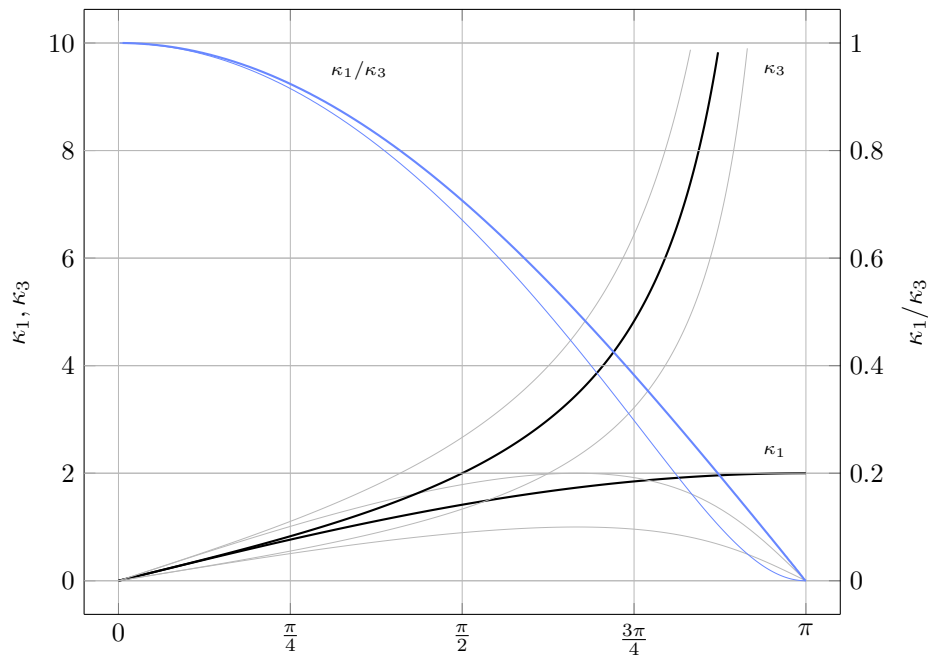


Figure 3.10 – Sensitivity of discrete curvatures to non uniform discretization ($\alpha \in [0.5, 2]$) over the whole domain of variation of the turning angle ($\varphi \in [0, \pi]$).

case of uniform discretization ($\alpha = 1$), whereas the thin lines mark the boundary cases ($\alpha = 0.5, 2$). The ratio κ_1/κ_3 is plotted in blue and leads to only one thin line (remind eq. (3.68)). The graph shows that κ_1 and κ_3 have a very close behavior for small turning angles. The variability regarding α is small when φ remains small and gets negligible as φ gets smaller.

Passing $\pi/4$ and increasing φ , κ_3 exhibits a good behavior : as the discrete curves tends to kink, κ_3 diverges towards the infinity as the smooth curvature would behave when the curve kinks. Conversely, the behavior of κ_1 is not appropriate as it converges to a fixed limit. This limit equals 2 when the edges have the same length and equals 0 when they have different lengths.

Conclusion

It appears that the discrete curvature related to the inscribed osculating circle exhibits a better behavior – that is a behavior closer to the smooth case – on the whole range of possible turning angles. This would be an advantage when modeling highly nonlinear beam configurations such as the ones encountered in hair simulations.

However, for the kind of structures we are studying here, those kind of configurations are not likely to arise. And if they do, the structure would be severely damaged and this situation is to be avoided by the designers. More over, the sharpness of the discretization could be increased to reduce the value of the turning angles and stay in the range $[0, \pi/4]$ where the circumscribed curvature gives accurate results.

3.7.3 Benchmarking : accuracy in bending energy representation

In this section we compare, for three remarkable types of curves (line, semicircle and elastica), the discrete bending energies \mathcal{E}_1 and \mathcal{E}_3 of the discrete curve, respectively based on definitions κ_1 and κ_3 (see tab. 3.1), to the bending energy \mathcal{E} of the smooth curve. We study the convergence of these energies as the sharpness of the discretization increases. The smooth and discrete bending energies are defined as :

$$\mathcal{E} = \int_0^L \kappa^2 ds \quad (3.69a)$$

$$\mathcal{E}_i = \sum_i \bar{l}_i \kappa_i^2 \quad (3.69b)$$

Straight line

Lets consider any straight line. Its smooth curvature is null. So are the discrete curvatures κ_1 and κ_3 (see tab. 3.1). In this case, the discrete bending energies perfectly match the bending energy of the smooth curve :

$$\mathcal{E} = \mathcal{E}_1 = \mathcal{E}_3 = 0 \quad (3.70)$$

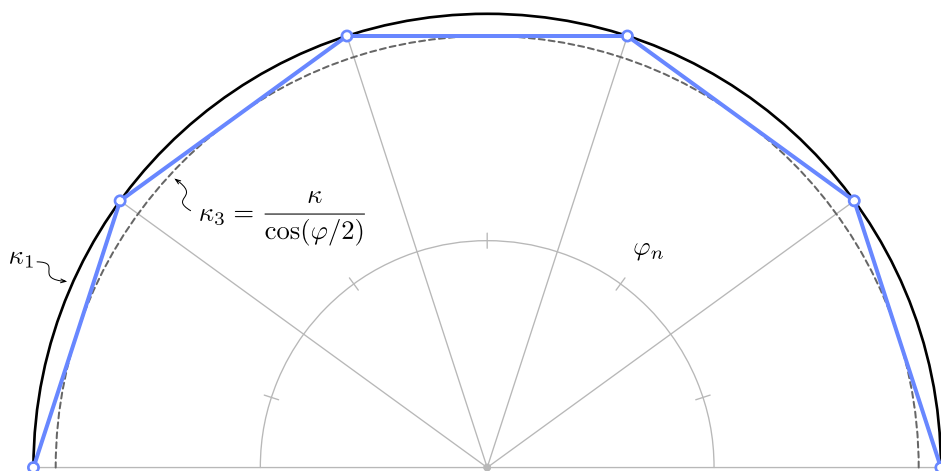
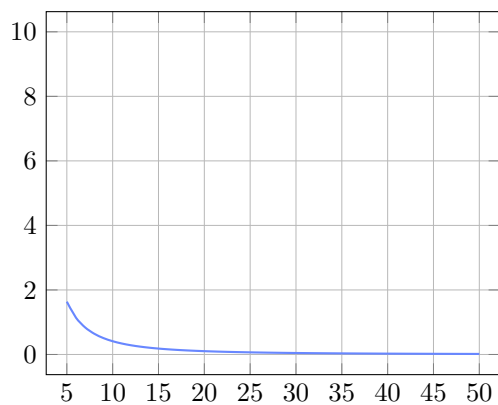
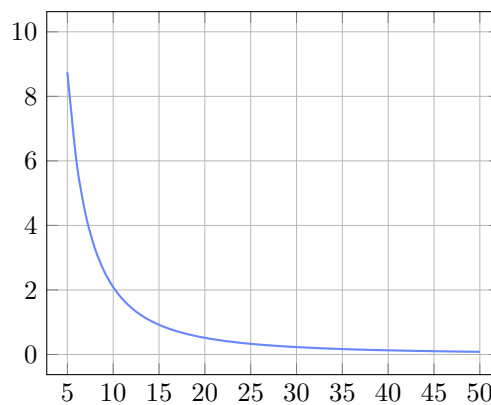


Figure 3.11 – Discretization of a semicircle and evaluation of its bending energy.

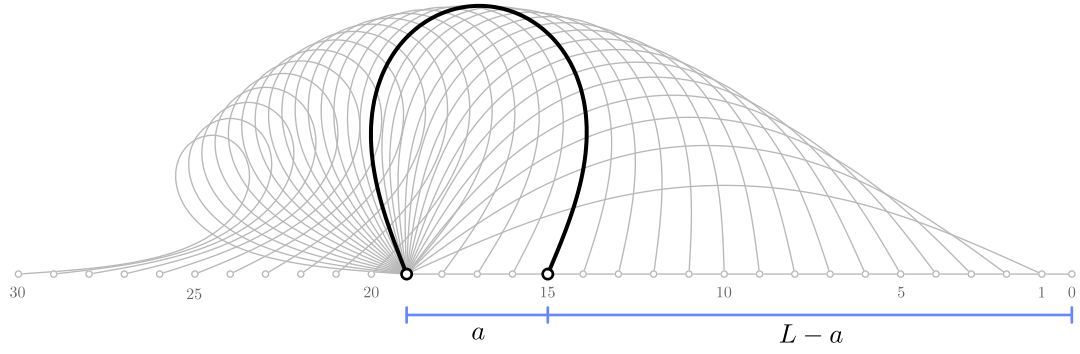


(a) $|1 - \frac{\mathcal{E}_1}{\mathcal{E}}(n)|$ in %

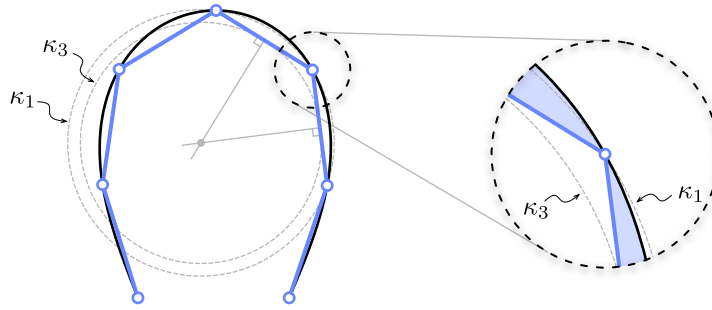


(b) $|1 - \frac{\mathcal{E}_3}{\mathcal{E}}(n)|$ in %

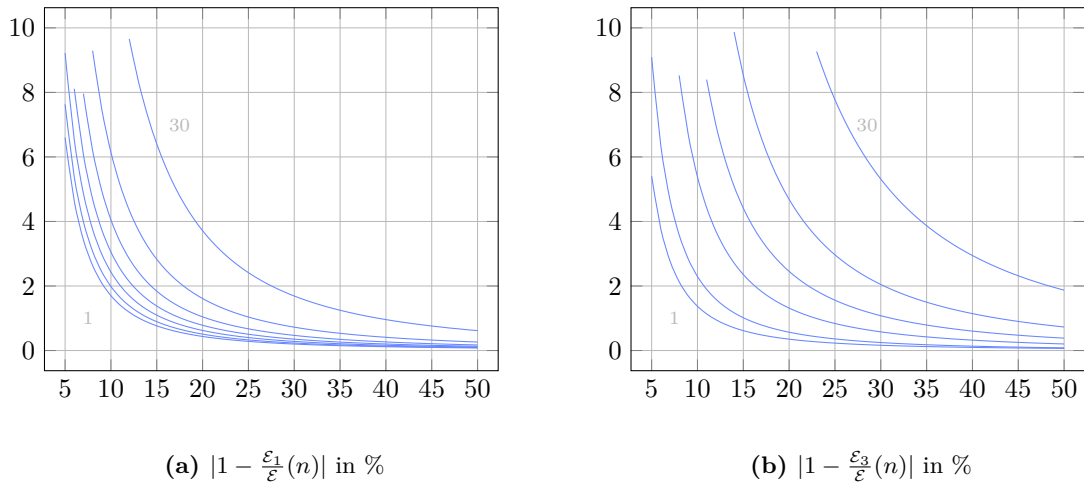
Figure 3.12 – Relative error in the estimation of the bending energy of a semicircle (\mathcal{E}) by the discrete energies \mathcal{E}_1 and \mathcal{E}_3 , regarding the sharpness of the discretization.



(a) sequence of elastica curves



(b) zoom on the discretization

Figure 3.13 – Discretization of an elastica curve and evaluation of its bending energy.

Figure 3.14 – Relative error in the estimation of the bending energy of an elastica (ε) by the discrete energies ε_1 and ε_3 , regarding the sharpness of the discretization. The curves (1,5,10,15,20,25,30) are chosen from [fig. 3.13a](#).

Semicircle

Lets consider a semicircle of curvature $\kappa = 1/r$ and length $L = \pi r$. This curve is discretized into n edges of equal length $|e_n| = 2r \sin(\varphi/2)$ where $\varphi = \frac{\pi}{n}$ (see [fig. 3.11](#)). The total length of the discrete curve is given by : $L_n = n|e_n| = L \frac{\sin(\varphi/2)}{\varphi/2}$. In this simple case, the bending energies can be expressed analytically :

$$\mathcal{E} = L\kappa^2 \quad (3.71a)$$

$$\mathcal{E}_1 = L_n \kappa_1^2 = \frac{\sin(\varphi/2)}{\varphi/2} \cdot \mathcal{E} \quad (3.71b)$$

$$\mathcal{E}_3 = L_n \kappa_3^2 = \frac{\sin(\varphi/2)}{(\varphi/2) \cos^2(\varphi/2)} \cdot \mathcal{E} \quad (3.71c)$$

Note that κ_1 equals the curvature of the smooth curve. Consequently, the estimation error is only due to the estimation of the curve length ($L_n \neq L$). The ratios $\mathcal{E}_1/\mathcal{E}$ and $\mathcal{E}_3/\mathcal{E}$ are plotted in [fig. 3.12](#). Graphs show that \mathcal{E}_1 converges to the smooth case faster than \mathcal{E}_3 .

Elastica

Lets consider a sequence of elastica curves of fixed length L and variable curvature κ (see [fig. 3.13a](#)). This curves correspond to a buckled shape of a straight pinned-pinned beam that would have been forced to retract its span. These curves are discretized into n edges of equal length (see [fig. 3.13b](#)). This time, there is no analytical expressions available for \mathcal{E} , \mathcal{E}_1 and \mathcal{E}_3 . Results are obtained by numerical integration and plotted in [fig. 3.14](#). Again, graphs show that \mathcal{E}_1 converges to the smooth case faster than \mathcal{E}_3 for most of the curves excepted the ones with low overall curvature (1 to 5).

Conclusion

[figures 3.12](#) and [3.14](#) show that for typical curves of mechanical interest – a semicircle is the shape of a rod with constant bending moment while the elastica is the shape of a buckled rod with no end moments – the circumscribed curvature gives a better approximation of the bending energy embedded in these curves. Hence, the circumscribed curvature seems to be a good candidate to maximize accuracy while minimizing the sampling of beam elements. This will lead to models with fewer nodes and decrease the cost of the computation.

3.8 Discrete tangent vector

In this section we study how to define the discrete unit tangent vector relatively to a discrete curve. While a natural definition exists along the edges (see [§3.6.1](#)), there is no obvious choice at vertices were the curve kinks.

The ability to define a unique tangent vector is very important to define the normal of cross-sections, to control beam endings, and to relate it to curvature. You would control

the direction of the section (for a fixed/encastre support condition) or conversly, you would control the moment and seek the corresponding tangent direction (for a pin boundary condition, you know there is no end moments so the curvature is null and you are looking for the tangent).

3.8.1 Circumscribed case

We consider the case where the curvature is defined according to the circumscribed osculating circle (see [fig. 3.15a](#)).

Current portion

Let \mathbf{x}_i be a vertex in the current portion of Γ . The circumscribed osculating circle gives a smooth approximation of Γ in the vicinity of \mathbf{x}_i (see [fig. 3.15a](#)). It leads to a natural definition of a unit tangent vector for five remarkable vertices as the tangent to the osculating circle at those points (resp. \mathbf{x}_{i-1} , $\mathbf{x}_{i-1/2}$, \mathbf{x}_i , $\mathbf{x}_{i+1/2}$, \mathbf{x}_{i+1}) :

$$\mathbf{t}_i^- = 2(\mathbf{t}_i \cdot \mathbf{u}_{i-1})\mathbf{u}_{i-1} - \mathbf{t}_i \quad (3.72a)$$

$$\mathbf{t}_{i-1/2} = \mathbf{u}_{i-1} \quad (3.72b)$$

$$\mathbf{t}_i = \frac{\|\mathbf{e}_i\|}{\|\mathbf{e}_{i-1} + \mathbf{e}_i\|}\mathbf{u}_{i-1} + \frac{\|\mathbf{e}_{i-1}\|}{\|\mathbf{e}_{i-1} + \mathbf{e}_i\|}\mathbf{u}_i \quad (3.72c)$$

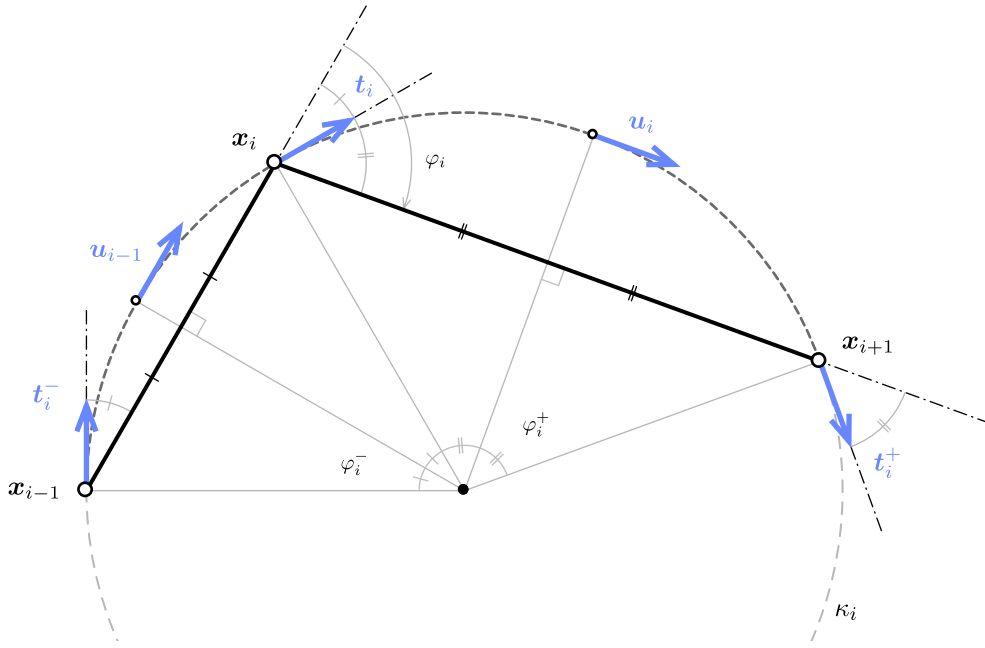
$$\mathbf{t}_{i+1/2} = \mathbf{u}_i \quad (3.72d)$$

$$\mathbf{t}_i^+ = 2(\mathbf{t}_i \cdot \mathbf{u}_i)\mathbf{u}_i - \mathbf{t}_i \quad (3.72e)$$

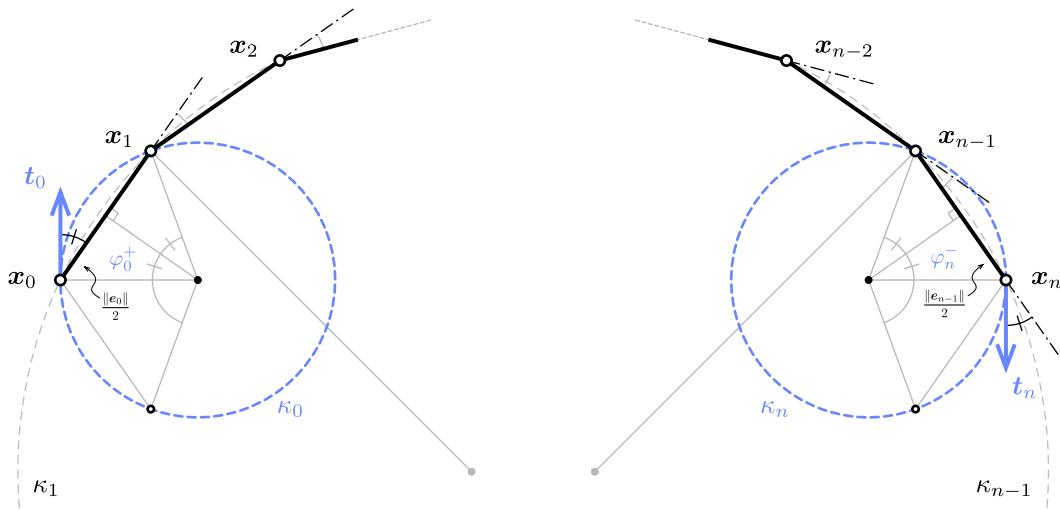
Note that \mathbf{t}_i^- (resp. \mathbf{t}_i^+) is obtained by a reflection of $-\mathbf{t}_i$ across the bisecting plane of \mathbf{e}_{i-1} (resp. \mathbf{e}_i). A very important property is that the curvature binormal vector at \mathbf{x}_i can be computed by three different ways :

$$\kappa \mathbf{b}_i = \frac{2 \mathbf{e}_{i-1} \times \mathbf{e}_i}{\|\mathbf{e}_{i-1}\| \|\mathbf{e}_i\| \|\mathbf{e}_{i-1} + \mathbf{e}_i\|} = \begin{cases} \frac{2 \mathbf{u}_{i-1} \times \mathbf{t}_i}{\|\mathbf{e}_{i-1}\|} \\ \frac{2 \mathbf{t}_i \times \mathbf{u}_i}{\|\mathbf{e}_i\|} \end{cases} \quad (3.73)$$

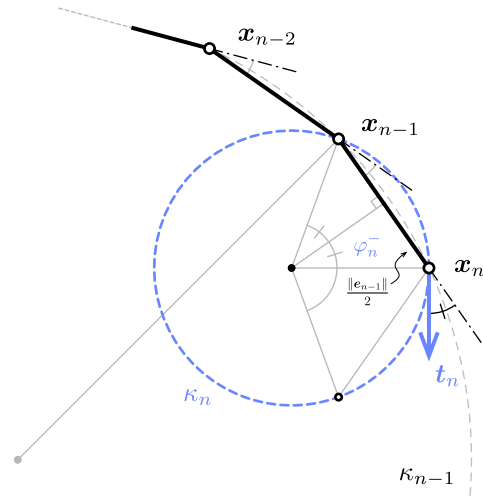
The first expression is interpreted as the unique circle passing through three points (\mathbf{x}_{i-1} , \mathbf{x}_i , \mathbf{x}_{i+1}) as explained in §3.7.1. Equivalently, there exist a unique circle defined by two points and a tangent vector. Precisely, the last two expressions in [eq. \(3.73\)](#) can be interpreted as the curvature binormal vector of the unique circle passing through \mathbf{x}_{i-1} , \mathbf{x}_i (resp. \mathbf{x}_i , \mathbf{x}_{i+1}) and tangent to \mathbf{t}_i at \mathbf{x}_i .



(a) current portion



(b) start



(c) end

Figure 3.15 – Definition of the tangent vector (\mathbf{t}) and related curvature binormal vector ($\kappa\mathbf{b}$) at vertices associated to the circumscribed curvature.

Discontinuity of curvature

Let \mathbf{t}_i^* be an arbitrary tangent vector at \mathbf{x}_i . Following [eq. \(3.73\)](#) we define the *left-sided* (resp. *right-sided*) discrete curvatures at \mathbf{x}_i in the circumscribed case as :

$$\kappa \mathbf{b}_i^-(\mathbf{t}_i^*) = \frac{2 \mathbf{u}_{i-1} \times \mathbf{t}_i^*}{\|\mathbf{e}_{i-1}\|} \quad (3.74a)$$

$$\kappa \mathbf{b}_i^+(\mathbf{t}_i^*) = \frac{2 \mathbf{t}_i^* \times \mathbf{u}_i}{\|\mathbf{e}_i\|} \quad (3.74b)$$

The corresponding osculating circle will be called the *left-sided* (resp. *right-sided*) circumscribed osculating circle. When $\mathbf{t}_i^* = \mathbf{t}_i$, the limits agree one to each other ($\kappa \mathbf{b}_i^- = \kappa \mathbf{b}_i^+ = \kappa \mathbf{b}_i$) and the osculating circles coincide. These definitions perfectly mimic the smooth case where, at a regular ($\|\gamma'\| \neq 0$) but not biregular ($\|\gamma''\| = 0$) point, the curvature is discontinuous while the tangent vector remains smoothly defined.

In mechanics, this situation is likely to arise as discontinuities in material properties or punctual applied moments will necessarily lead to discontinuities in curvature (recall that $M = EI\kappa$).

Curve endings

The definition of the left and right sided curvatures given for a vertex in the current portion of Γ are still valid for the end vertices \mathbf{x}_0 and \mathbf{x}_n . Provided that a unit tangent vector \mathbf{t}_0^* (respectively \mathbf{t}_n^*) is given at \mathbf{x}_0 (resp. \mathbf{x}_n), the circumscribed osculating circle is defined as the unique circle passing through \mathbf{x}_0 and \mathbf{x}_1 (resp. \mathbf{x}_{n-1} and \mathbf{x}_n) tangent to \mathbf{t}_0^* (resp. \mathbf{t}_n^*) ; see [fig. 3.15b](#) and [fig. 3.15c](#). It leads to the following curvature binormal vectors :

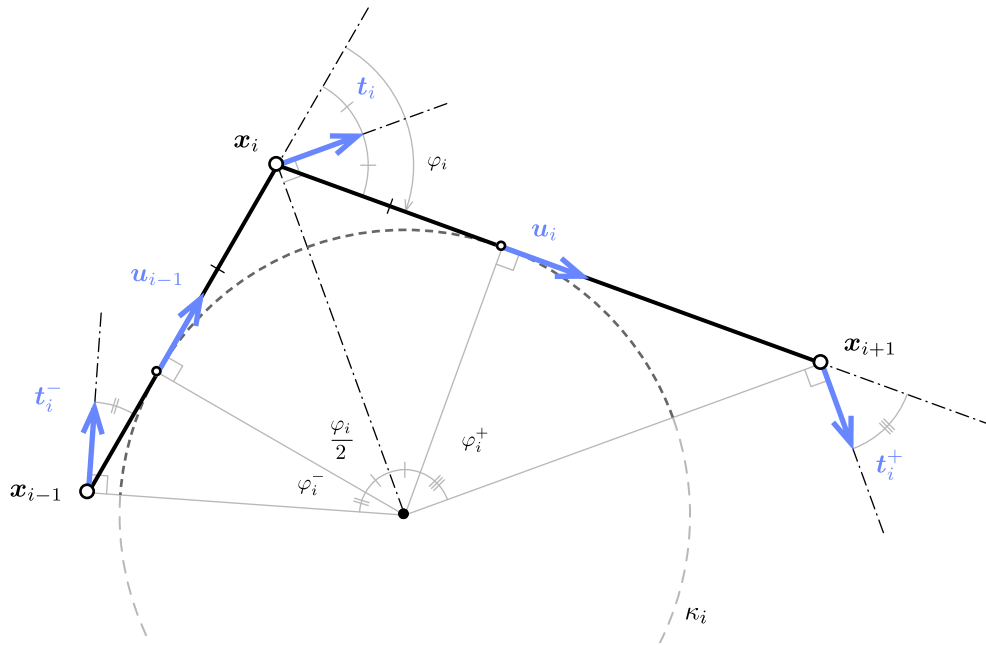
$$\kappa \mathbf{b}_0 = \kappa \mathbf{b}_0^+(\mathbf{t}_0^*) = \frac{2 \mathbf{t}_0^* \times \mathbf{e}_0}{\|\mathbf{e}_0\|^2} \quad (3.75a)$$

$$\kappa \mathbf{b}_n = \kappa \mathbf{b}_n^-(\mathbf{t}_n^*) = \frac{2 \mathbf{e}_{n-1} \times \mathbf{t}_n^*}{\|\mathbf{e}_{n-1}\|^2} \quad (3.75b)$$

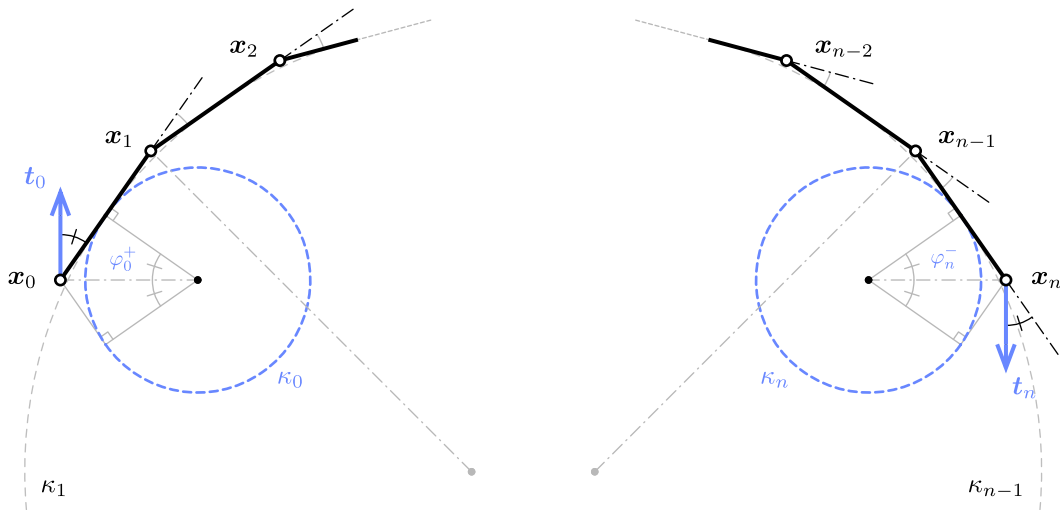
Note that, contrary to the current portion, curvatures at endings are subjected to the definition of a unit tangent vector. This reflects the usual indetermination of boundary conditions. For a given beam whether the end is clamped and the tangent vector is known and one will seek the reacting moment due to the support ; whether the end is pinned and the reacting moment is null (so is the curvature) and one will seek the cross-section orientation.

3.8.2 Inscribed case

We now consider the case where the curvature is defined according to the inscribed osculating circle (see [fig. 3.16a](#)). Remark that inscribed and circumscribed osculating circles are concentric when $l_{i-1} = l_i$.



(a) current portion



(b) start

(c) end

Figure 3.16 – Definition of the tangent vector (\mathbf{t}) and related curvature binormal vector ($\kappa\mathbf{b}$) at vertices associated to the inscribed curvature.

Current portion

Let \mathbf{x}_i be a vertex in the current portion of Γ . The inscribed osculating circle gives a smooth approximation of Γ in the vicinity of \mathbf{x}_i (see [fig. 3.16a](#)) ; though this approximation does not pass through the vertices. It is again possible to construct some unit tangent vectors based on this circle, but the analytic expressions are less compact than in the circumscribed case (resp. at \mathbf{x}_{i-1} , \mathbf{x}_i , \mathbf{x}_{i+1}) :

$$\mathbf{t}_i^- = \cos\left(\frac{\varphi_i}{2} + \varphi_i^-\right) \frac{\mathbf{u}_{i-1} + \mathbf{u}_i}{\|\mathbf{u}_{i-1} + \mathbf{u}_i\|} + \sin\left(\frac{\varphi_i}{2} + \varphi_i^-\right) \frac{\mathbf{u}_{i-1} - \mathbf{u}_i}{\|\mathbf{u}_{i-1} - \mathbf{u}_i\|} \quad (3.76a)$$

$$\mathbf{t}_i = \frac{\mathbf{u}_{i-1} + \mathbf{u}_i}{\|\mathbf{u}_{i-1} + \mathbf{u}_i\|} \quad (3.76b)$$

$$\mathbf{t}_i^+ = \cos\left(\frac{\varphi_i}{2} + \varphi_i^+\right) \frac{\mathbf{u}_{i-1} + \mathbf{u}_i}{\|\mathbf{u}_{i-1} + \mathbf{u}_i\|} - \sin\left(\frac{\varphi_i}{2} + \varphi_i^+\right) \frac{\mathbf{u}_{i-1} - \mathbf{u}_i}{\|\mathbf{u}_{i-1} - \mathbf{u}_i\|} \quad (3.76c)$$

In this form, the expressions of \mathbf{t}_i^- and \mathbf{t}_i^+ exhibit lots of trigonometric computations. Consequently, they will be more costly to evaluate (numerically) than the ones given for the circumscribed case that exhibit only simple addition, product and division operations.

Though these points does not generally fall into mid-edge, the tangent vector can also be identified to \mathbf{u}_{i-1} (resp. \mathbf{u}_i) at point $\tilde{\mathbf{x}}_i^- = \mathbf{x}_i - \frac{1}{2}\bar{l}_i\mathbf{u}_{i-1}$ (resp. $\tilde{\mathbf{x}}_i^+ = \mathbf{x}_i + \frac{1}{2}\bar{l}_i\mathbf{u}_i$) :

$$\tilde{\mathbf{t}}_i^- = \mathbf{u}_{i-1} \quad (3.77a)$$

$$\tilde{\mathbf{t}}_i^+ = \mathbf{u}_i \quad (3.77b)$$

Similarly to the circumscribed case, one can remark that the curvature binormal vector at \mathbf{x}_i can be computed in three different manners :

$$\kappa \mathbf{b}_i = \frac{2}{\bar{l}_i} \left(\frac{\mathbf{e}_{i-1} \times \mathbf{e}_i}{\|\mathbf{e}_{i-1}\| \|\mathbf{e}_i\| + \mathbf{e}_{i-1} \cdot \mathbf{e}_i} \right) = \begin{cases} \frac{2}{\bar{l}_i} \left(\frac{\mathbf{e}_{i-1} \times \mathbf{t}_i}{\mathbf{e}_{i-1} \cdot \mathbf{t}_i} \right) \\ \frac{2}{\bar{l}_i} \left(\frac{\mathbf{t}_i \times \mathbf{e}_i}{\mathbf{t}_i \cdot \mathbf{e}_i} \right) \end{cases} \quad (3.78)$$

The first expression is interpreted as the unique circle bitangent to \mathbf{e}_{i-1} at $\tilde{\mathbf{x}}_i^-$ and \mathbf{e}_i at $\tilde{\mathbf{x}}_i^+$, as explained in [§3.7.1](#). Equivalently, the last two expressions in [eq. \(3.78\)](#) can be interpreted as the curvature binormal vector of the unique circle which center is on the line normal to \mathbf{t}_i passing through \mathbf{x}_i , and that is tangent to \mathbf{e}_{i-1} (resp. \mathbf{e}_i) at $\tilde{\mathbf{x}}_i^-$ (resp. $\tilde{\mathbf{x}}_i^+$).

Discontinuity of curvature

Let \mathbf{t}_i^* be an arbitrary tangent vector at \mathbf{x}_i . Following [eq. \(3.78\)](#) we define the *left-sided* (resp. *right-sided*) discrete curvature at \mathbf{x}_i in the inscribed case as :

$$\kappa \mathbf{b}_i^-(\mathbf{t}_i^*) = \frac{2}{\bar{l}_i} \left(\frac{\mathbf{e}_{i-1} \times \mathbf{t}_i^*}{\mathbf{e}_{i-1} \cdot \mathbf{t}_i^*} \right) \quad (3.79a)$$

$$\kappa \mathbf{b}_i^+(\mathbf{t}_i^*) = \frac{2}{\bar{l}_i} \left(\frac{\mathbf{t}_i^* \times \mathbf{e}_i}{\mathbf{t}_i^* \cdot \mathbf{e}_i} \right) \quad (3.79b)$$

The corresponding osculating circle will be called the *left-sided* (resp. *right-sided*) inscribed osculating circle. When $\mathbf{t}_i^* = \mathbf{t}_i$, the limits agree one to each other ($\kappa \mathbf{b}_i^- = \kappa \mathbf{b}_i^+ = \kappa \mathbf{b}_i$) and the osculating circles coincide. These definitions perfectly mimic the smooth case where, at a regular ($\|\gamma'\| \neq 0$) but not biregular ($\|\gamma''\| = 0$) point, the curvature is discontinuous while the tangent vector remains smoothly defined.

Curve endings

The definition of the left and right sided curvatures given for a vertex in the current portion of Γ are still valid for the end vertices \mathbf{x}_0 and \mathbf{x}_n . Provided that a unit tangent vector \mathbf{t}_0^* (respectively \mathbf{t}_n^*) is given at \mathbf{x}_0 (resp. \mathbf{x}_n), the circumscribed osculating circle is defined as the unique circle passing through \mathbf{x}_0 and \mathbf{x}_1 (resp. \mathbf{x}_{n-1} and \mathbf{x}_n) tangent to \mathbf{t}_0^* (resp. \mathbf{t}_n^*) ; see [fig. 3.16b](#) and [fig. 3.16c](#). It leads to the following curvature binormal vectors :

$$\kappa \mathbf{b}_0 = \kappa \mathbf{b}_0^+(\mathbf{t}_0^*) = \frac{2}{\|\mathbf{e}_0\|} \left(\frac{\mathbf{t}_0^* \times \mathbf{e}_0}{\mathbf{t}_0^* \cdot \mathbf{e}_0} \right) \quad (3.80a)$$

$$\kappa \mathbf{b}_n = \kappa \mathbf{b}_n^-(\mathbf{t}_n^*) = \frac{2}{\|\mathbf{e}_{n-1}\|} \left(\frac{\mathbf{e}_{n-1} \times \mathbf{t}_n^*}{\mathbf{e}_{n-1} \cdot \mathbf{t}_n^*} \right) \quad (3.80b)$$

Note that, contrary to the current portion, curvatures at endings are subjected to the definition of a unit tangent vector. This reflects the usual indetermination of boundary conditions. For a given beam whether the end is clamped, the tangent vector is known and one will seek the reacting moment due to the support ; whether the end is pinned, the reacting moment is null (so is the curvature) and one will seek the cross-section orientation.

Conclusion

We have extended the comprehension of the discrete curvature to the extremities of the curve, for both the circumscribed and inscribed definitions of the discrete curvature. We have seen that these notions lead to a natural definition of the tangent at vertices in the current portion as at the extremities.

When the curvature is prescribed at a given vertex, [eq. \(3.74a\)](#) and [\(3.74b\)](#) (circumscribed) or [eq. \(3.79a\)](#) and [\(3.79b\)](#) (inscribed) need to be solved to determine the tangent vector. Remark that both systems are linear in \mathbf{t} .

3.9 Discrete parallel transport

Discrete parallel transport can be computed by analogy to the smooth case as the minimal rotation around \mathbf{t} . However, this method gets unstable when \mathbf{t}_i and \mathbf{t}_{i+1} get almost collinear because of the cross product (although the rotation angle tends to zero, the rotation axis become very sensitive to numerical instabilities).

Note that while these definitions of parallel transport are illustrated to transport vectors in space from one location $\{\mathbf{x}, \mathbf{t}\}(s)$ to another $\{\mathbf{x}, \mathbf{t}\}(s + ds)$, it is identically transposed to parallel transport in time from one location $\{\mathbf{x}, \mathbf{t}\}(t)$ to another $\{\mathbf{x}, \mathbf{t}\}(t + dt)$ as suggested in [25].

3.9.1 The rotation method

The rotation method is given by Bloomenthal 1990 [8]. First, the frame at \mathbf{x}_i is simply translated at vertex \mathbf{x}_{i+1} . Then, the translated frame is rotated so that \mathbf{t}_i aligns with \mathbf{t}_{i+1} . The rotation axis is chosen to be $\mathbf{b} = \mathbf{t}_i \times \mathbf{t}_{i+1}$ and the angle of rotation is denoted α (see fig. 3.17a). This is analogous to the smooth case.

3.9.2 The double reflexion method

The double reflection method is given by Wang et al. 2008 [11]. It is supposed to be of order $o(h^4)$ whereas the rotation method is only $o(h^2)$, where $h = \sup_{i \in \llbracket 0, n \rrbracket} \|\mathbf{e}_i\|$ is the sharpness of the discretization. Though their computation cost is quite similar, the double reflection method is not subject to instability when \mathbf{t}_i and \mathbf{t}_{i+1} tend to be collinear, which is an obvious advantage.

We denote \mathcal{R}_x^n the reflection across the plane passing through the point \mathbf{x} and normal to the unit vector $\mathbf{n} = \mathbf{e}_i / \|\mathbf{e}_i\|$. Thus, \mathbf{v} is mapped through \mathcal{R} into $\mathbf{v}^* = \mathbf{v} - 2(\mathbf{v} \cdot \mathbf{n})\mathbf{n}$.

Let $\mathcal{R}_1 = \mathcal{R}_{\mathbf{x}_{i+1/2}}^{n_1}$ be the reflection across the bisecting plane of \mathbf{e}_i ($\mathbf{n}_1 = \mathbf{u}_i$). Let $\mathbf{t}_i^* = \mathcal{R}_1(\mathbf{t}_i)$ be the image of \mathbf{t}_i by \mathcal{R}_1 . Let $\mathcal{R}_2 = \mathcal{R}_{\mathbf{x}_{i+1}}^{n_2}$ be the reflection across the bisecting plane of the points $\mathbf{x}_{i+1} + \mathbf{t}_i^*$ and $\mathbf{x}_{i+1} + \mathbf{t}_{i+1}$. Thus, $\mathbf{n}_2 = \frac{\mathbf{t}_{i+1} - \mathbf{t}_i^*}{\|\mathbf{t}_{i+1} - \mathbf{t}_i^*\|}$ (see fig. 3.17b).

Parallel transport is defined as the *double reflection* through \mathcal{R}_1 and \mathcal{R}_2 :

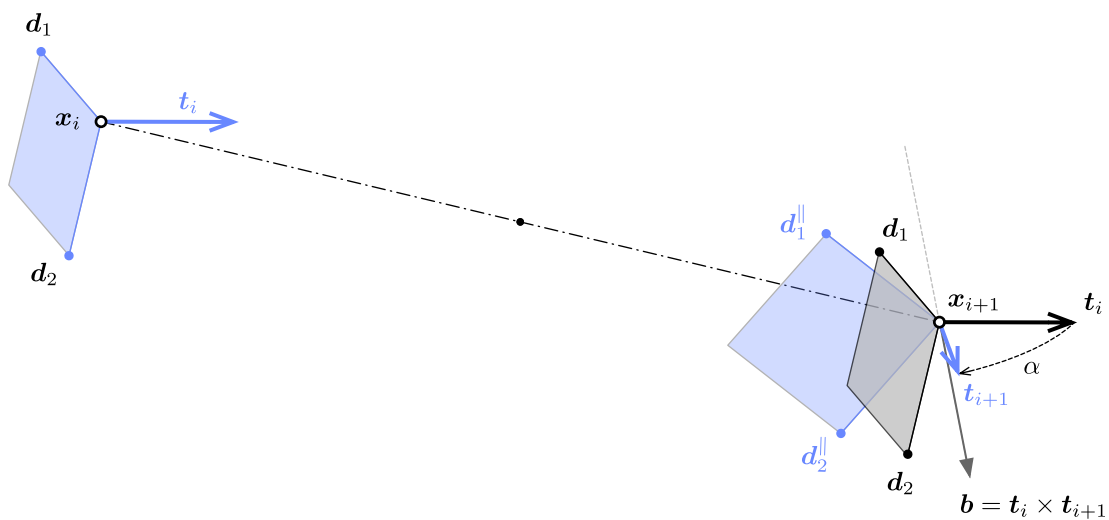
$$\mathcal{P}_{\{\mathbf{x}_i, \mathbf{t}_i\}}^{\{\mathbf{x}_{i+1}, \mathbf{t}_{i+1}\}} = \mathcal{P}_i^{i+1} = \mathcal{R}_2 \circ \mathcal{R}_1 \quad (3.81)$$

Let $\mathcal{F}_i = \{\mathbf{t}_i, \mathbf{d}_1, \mathbf{d}_2\}$ be an orthonormal frame at \mathbf{x}_i . Let $\mathcal{F}_i^* = \mathcal{R}_1(\mathcal{F}_i) = \{\mathbf{t}_i^*, \mathbf{d}_1^*, \mathbf{d}_2^*\}$ be the image of \mathcal{F}_i by \mathcal{R}_1 . Then :

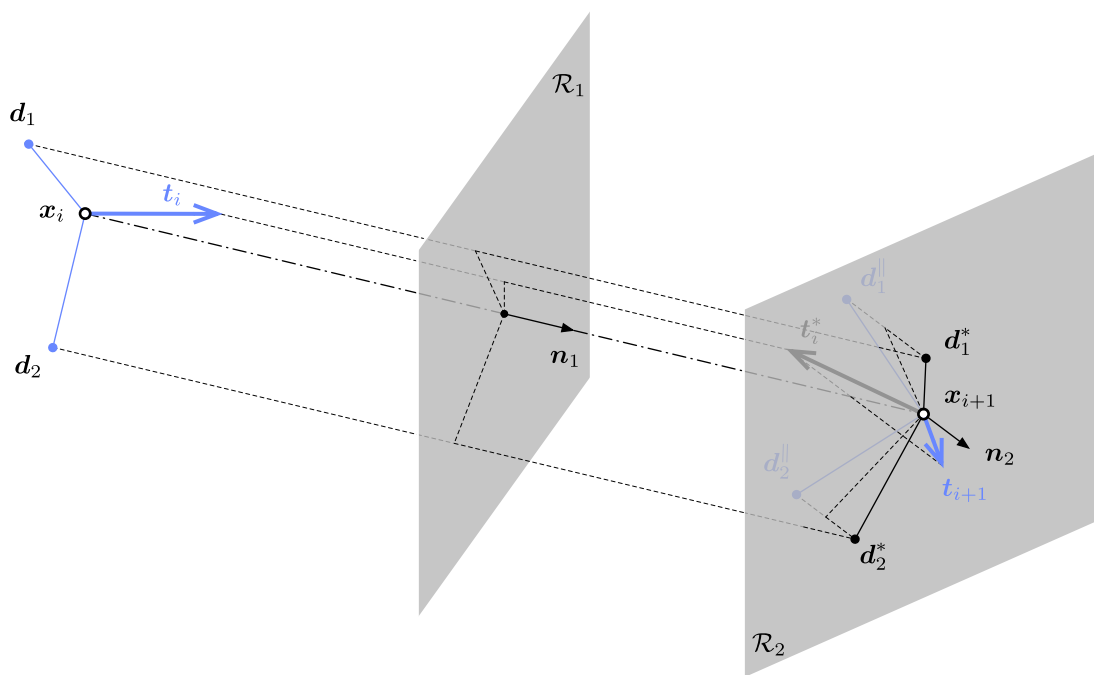
$$\mathbf{t}_i^* = \mathbf{t}_i - 2(\mathbf{t}_i \cdot \mathbf{n}_1)\mathbf{n}_1 \quad (3.82a)$$

$$\mathbf{d}_1^* = \mathbf{d}_1 - 2(\mathbf{d}_1 \cdot \mathbf{n}_1)\mathbf{n}_1 \quad (3.82b)$$

$$\mathbf{d}_2^* = \mathbf{d}_1^* \times \mathbf{t}_i^* \quad (3.82c)$$



(a) rotation method



(b) double reflection method

Figure 3.17 – Two methods to parallel transport a vector from $\{x_i, t_i\}$ to $\{x_{i+1}, t_{i+1}\}$.

Let $\mathcal{F}_i^\parallel = \mathcal{R}_2(\mathcal{F}_i^*) = \{\mathbf{t}_{i+1}, \mathbf{d}_1^\parallel, \mathbf{d}_2^\parallel\}$ be the image of \mathcal{F}_i^* by \mathcal{R}_2 . Then the parallel transported vectors are given by :

$$\mathbf{d}_1^\parallel = \mathbf{d}_1^* - 2(\mathbf{d}_1^* \cdot \mathbf{n}_2)\mathbf{n}_2 \quad (3.83a)$$

$$\mathbf{d}_2^\parallel = \mathbf{t}_{i+1} \times \mathbf{d}_1^\parallel \quad (3.83b)$$

The double reflection is equivalent to a rotation around the line \mathcal{D} defined as the intersection of the two reflection planes, of direction $\mathbf{b} = \mathbf{n}_1 \times \mathbf{n}_2$, by an angle $\alpha = 2\angle(\mathbf{n}_1, \mathbf{n}_2) = 2\arcsin(\|\mathbf{b}\|)$.

Remark that for both the circumscribed (see [fig. 3.15a](#)) and inscribed (see [fig. 3.16a](#)) osculating circles :

$$\mathbf{t}_i = \mathcal{R}_{\mathbf{x}_{i-1/2}}^{u_{i-1}} \circ \mathcal{R}_{\mathbf{x}_i}^{t_i}(\mathbf{t}_i^-) \quad (3.84a)$$

$$\mathbf{t}_i = \mathcal{R}_{\mathbf{x}_i}^{t_i} \circ \mathcal{R}_{\mathbf{x}_{i+1/2}}^{u_i}(\mathbf{t}_i^+) \quad (3.84b)$$

3.10 Conclusion

This chapter has established all the geometrical tools required for our future discrete beam model. Our analysis show that for the type of structures we want to model the discrete curvature defined according to the circumscribed osculating circle is the most suitable as :

- it provides an unequivocal definition of the discrete curvature in the current portion and at the extremities of the curve ;
- it exhibits the fastest convergence when regarding the evaluation of the bending energy of typical curves ;
- it leads to a natural local spline interpolation passing through the curve's vertices ;
- it leads to a natural definition of the tangent vector at vertices and at midspan of edges ;
- it enables the modeling of curvature discontinuities.

3.11 References

- [1] G. F. A. de L'Hospital. "Analyse des infiniment petits, pour l'intelligence des lignes courbes". In: (1696).
- [2] J. Delcourt. "Analyse et géométrie, histoire des courbes gauches de Clairaut à Darboux". In: *Archive for History of Exact Sciences* 65.3 (2011), pp. 229–293.
- [3] T. Hoffmann. "Discrete Differential Geometry of Curves and Surfaces". In: 18 (2008).
- [4] E. Vouga. "Plane Curves". In: *Lectures in discrete differential geometry*. 2014. Chap. 1, pp. 1–11.
- [5] R. Bishop. "There is more than one way to frame a curve". In: *Mathematical Association of America* (1975).
- [6] F. Klok. "Two moving coordinate frames for sweeping along a 3D trajectory". In: *Computer Aided Geometric Design* 3.3 (1986), pp. 217–229.
- [7] H. Guggenheimer. "Computing frames along a trajectory". In: *Computer Aided Geometric Design* 6.1 (1989), pp. 77–78.
- [8] J. Bloomenthal. "Calculation of reference frames along a space curve". In: *Graphics Gems*. Ed. by A. S. Glassner. Vol. 1. San Diego, CA, USA: Academic Press Professional, Inc., 1990, pp. 567–571.
- [9] A. J. Hanson and H. Ma. *Parallel Transport Approach to Curve Framing*. Tech. rep. 1995.
- [10] T. Poston, S. Fang, and W. Lawton. "Computing and approximating sweeping surfaces based on rotation minimizing frames". In: *Proceedings of the 4th International Conference on CAD/CG*. 1995, pp. 1–8.
- [11] W. Wang, B. Jüttler, D. Zheng, and Y. Liu. "Computation of rotation minimizing frames". In: *ACM Transactions on Graphics* 27.1 (2008), pp. 1–18.
- [12] R. T. Farouki, C. Giannelli, M. L. Sampoli, and A. Sestini. "Rotation-minimizing osculating frames". In: *Computer Aided Geometric Design* 31.1 (2014), pp. 27–42.
- [13] F. Frenet. "Sur les courbes à double courbure". In: *Journal de Mathématiques Pures et Appliquées* 17 (1852), pp. 437–447.
- [14] J. Delcourt. "Analyse et géométrie : les courbes gauches de Clairaut à Serret". PhD thesis. Université de Paris VI, 2007, p. 302.
- [15] J. Bernoulli. *Johannis Bernoulli... Opera omnia, tam antea sparsim edita, quam hactenus inedita*. IV. sumptibus Marci-Michaelis Bousquet, 1728, p. 584.
- [16] H. Pitot. "Quadrature de la moitié d'une courbe des arcs appelée la compagne de la cycloïde". In: *Mémoires de l'Académie Royale des Sciences (1724)* (1726), pp. 107–113.
- [17] J. L. Coolidge. *A history of geometrical methods*. Ed. by C. Corporation. Dover Books on Mathematics. Dover Publications, 2013, p. 480.
- [18] G. Monge. *Application de l'analyse à la géométrie*. 1809, p. 475.

- [19] L. Euler. “Continens analysin, pro incuruatione fili in fingulis punctis inueniendia”. In: *Novi Commentarii academiae scientiarum Petropolitanae* 19 (1775), pp. 340–370.
- [20] A. Gray, E. Abbena, and S. Salamon. *Modern differential geometry of curves and surfaces with Mathematica*. Ed. by E. A. Salamon and Simon. Third. CRC Press, 2006, p. 1016.
- [21] M. Bergou, M. Wardetzky, S. Robinson, B. Audoly, and E. Grinspun. “Discrete elastic rods”. In: *ACM SIGGRAPH* (2008), pp. 1–12.
- [22] D. Carroll, E. Hankins, E. Kose, and I. Sterling. “A survey of the differential geometry of discrete curves”. In: *The Mathematical Intelligencer* 36.4 (2014), pp. 28–35. [arXiv:1311.5862v1](#).
- [23] A. Bobenko. *Discrete differential geometry*. Second. 2015, p. 144.
- [24] P. Romon. *Introduction à la géométrie différentielle discrète*. Références sciences. Ellipses, 2013, p. 216.
- [25] M. Bergou, B. Audoly, E. Vouga, M. Wardetzky, and E. Grinspun. “Discrete viscous threads”. In: *ACM Transactions on ...* (2010), pp. 1–10.